RECOMMENDATION ITU-R P.452-12*

Prediction procedure for the evaluation of microwave interference between stations on the surface of the Earth at frequencies above about 0.7 GHz**

(Question ITU-R 208/3)

(1970-1974-1978-1982-1986-1992-1994-1995-1997-1999-2001-2003-2005)

The ITU Radiocommunication Assembly,

considering

a) that due to congestion of the radio spectrum, frequency bands must be shared between different terrestrial services, between systems in the same service and between systems in the terrestrial and Earth-space services;

b) that for the satisfactory coexistence of systems sharing the same frequency bands, interference propagation prediction procedures are needed that are accurate and reliable in operation and acceptable to all parties concerned;

c) that interference propagation predictions are required to meet "worst-month" performance and availability objectives;

d) that prediction methods are required for application to all types of path in all areas of the world,

recommends

1 that the microwave interference prediction procedure given in Annex 1 be used for the evaluation of the available propagation loss in interference calculations between stations on the surface of the Earth for frequencies above about 0.7 GHz.

Annex 1

1 Introduction

Congestion of the radio-frequency spectrum has made necessary the sharing of many frequency bands between different radio services, and between the different operators of similar radio services. In order to ensure the satisfactory coexistence of the terrestrial and Earth-space systems involved, it is important to be able to predict with reasonable accuracy the interference potential between them, using prediction procedures and models which are acceptable to all parties concerned, and which have demonstrated accuracy and reliability.

---

* *Note by the BR Secretariat* – The footnote below was amended editorially in November 2006.

** A computer spreadsheet associated with the clear air prediction procedures described in this Recommendation is available from the ITU-R website dealing with Radiocommunication Study Group 3.

Many types and combinations of interference path may exist between stations on the surface of the Earth, and between these stations and stations in space, and prediction methods are required for each situation. This Annex addresses one of the more important sets of interference problems, i.e. those situations where there is a potential for interference between microwave radio stations located on the surface of the Earth.

The prediction procedure is appropriate to radio stations operating in the frequency range of about 0.7 GHz to 50 GHz. For median basic transmission losses the method is believed to be reliable at frequencies down to 0.1 GHz. However, the ducting model, which is important at low-time percentages, has not been tested to frequencies lower than about 0.7 GHz.

The method includes a complementary set of propagation models which ensure that the predictions embrace all the significant interference propagation mechanisms that can arise. Methods for analysing the radio-meteorological and topographical features of the path are provided so that predictions can be prepared for any practical interference path falling within the scope of the procedure up to a distance limit of 10 000 km.

2 Interference propagation mechanisms

Microwave interference may arise through a range of propagation mechanisms whose individual dominance depends on climate, radio frequency, time percentage of interest, distance and path topography. At any one time a single mechanism or more than one may be present. The principal interference propagation mechanisms are as follows:

– *Line-of-sight* (Fig. 1): The most straightforward interference propagation situation is when a line-of-sight transmission path exists under normal (i.e. well-mixed) atmospheric conditions. However, an additional complexity can come into play when subpath diffraction causes a slight increase in signal level above that normally expected. Also, on all but the shortest paths (i.e. paths longer than about 5 km) signal levels can often be significantly enhanced for short periods of time by multipath and focusing effects resulting from atmospheric stratification (see Fig. 2).

– *Diffraction* (Fig. 1): Beyond line-of-sight and under normal conditions, diffraction effects generally dominate wherever significant signal levels are to be found. For services where anomalous short-term problems are not important, the accuracy to which diffraction can be modelled generally determines the density of systems that can be achieved. The diffraction prediction capability must have sufficient utility to cover smooth-earth, discrete obstacle and irregular (unstructured) terrain situations.

– *Tropospheric scatter* (Fig. 1): This mechanism defines the “background” interference level for longer paths (e.g. more than 100-150 km) where the diffraction field becomes very weak. However, except for a few special cases involving sensitive earth stations or very high power interferers (e.g. radar systems), interference via troposcatter will be at too low a level to be significant.

– *Surface ducting* (Fig. 2): This is the most important short-term interference mechanism over water and in flat coastal land areas, and can give rise to high signal levels over long distances (more than 500 km over the sea). Such signals can exceed the equivalent “free-space” level under certain conditions.

FIGURE 1

Long-term interference propagation mechanisms

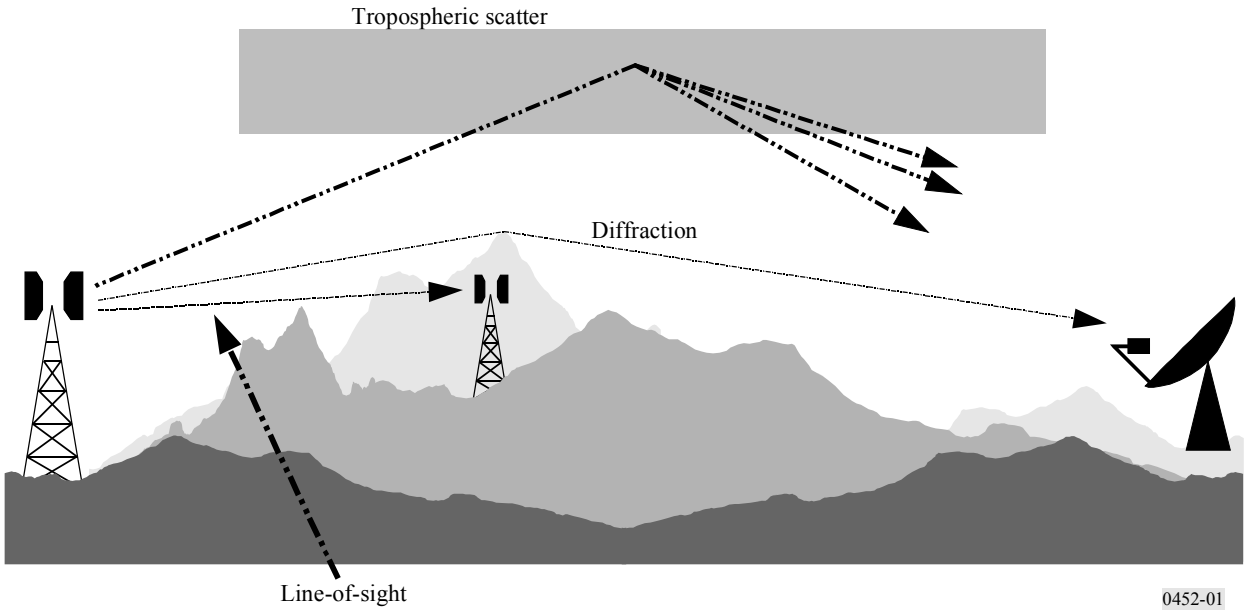

– *Elevated layer reflection and refraction* (Fig. 2): The treatment of reflection and/or refraction from layers at heights up to a few hundred metres is of major importance as these mechanisms enable signals to overcome the diffraction loss of the terrain very effectively under favourable path geometry situations. Again the impact can be significant over quite long distances (up to 250-300 km).

– *Hydrometeor scatter* (Fig. 2): Hydrometeor scatter can be a potential source of interference between terrestrial link transmitters and earth stations because it may act virtually omnidirectionally, and can therefore have an impact off the great-circle interference path. However, the interfering signal levels are quite low and do not usually represent a significant problem.

A basic problem in interference prediction (which is indeed common to all tropospheric prediction procedures) is the difficulty of providing a unified consistent set of practical methods covering a wide range of distances and time percentages; i.e. for the real atmosphere in which the statistics of dominance by one mechanism merge gradually into another as meteorological and/or path conditions change. Especially in these transitional regions, a given level of signal may occur for a total time percentage which is the sum of those in different mechanisms. The approach in this procedure has been deliberately to keep separate the prediction of interference levels from the different propagation mechanisms up to the point where they can be combined into an overall prediction for the path. This overall prediction is made using a blending technique that ensures for any given path distance and time percentage that the signal enhancement in the equivalent notional line-of-sight model is the highest attainable.

FIGURE 2

Anomalous (short-term) interference propagation mechanisms

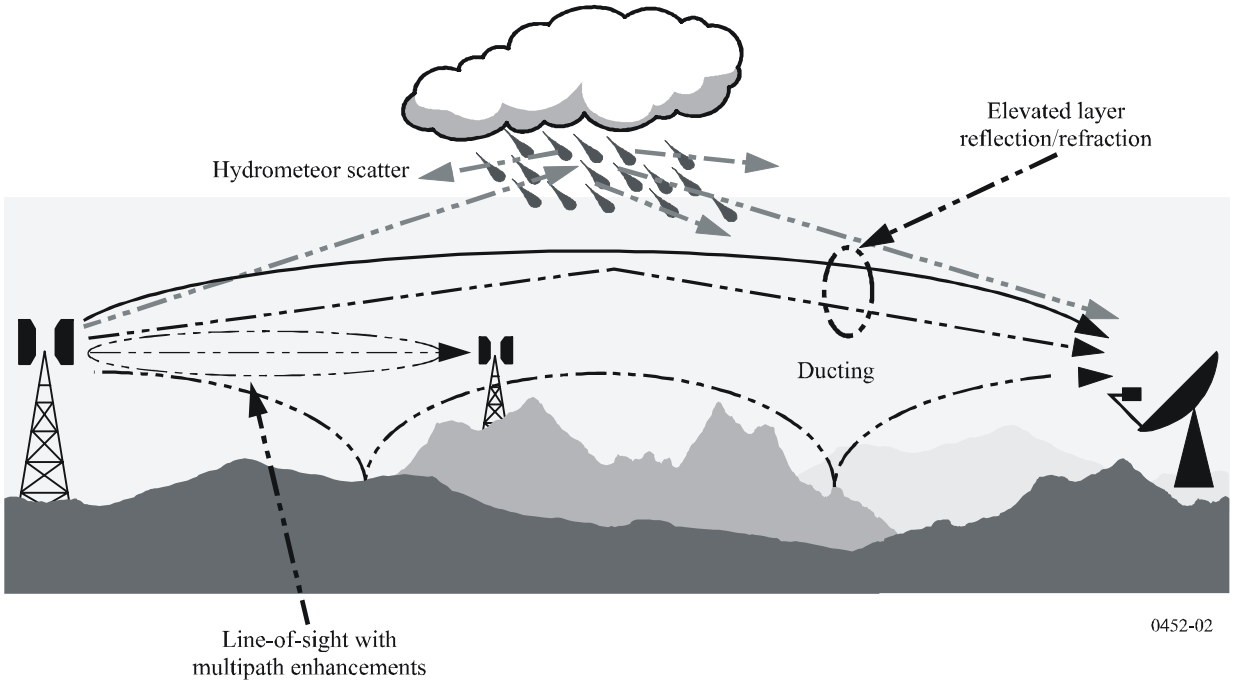

3 Clear-air interference prediction

3.1 General comments

The procedure uses five propagation models to deal with the clear-air propagation mechanisms described in § 2. These models are as follows:

– *line-of-sight* (including signal enhancements due to multipath and focusing effects);

– *diffraction* (embracing smooth-earth, irregular terrain and sub-path cases);

– *tropospheric scatter*;

– *anomalous propagation* (ducting and layer reflection/refraction);

– *height-gain variation in clutter* (where relevant).

Depending on the type of path, as determined by a path profile analysis, one or more of these models are exercised in order to provide the required prediction of basic transmission loss.

3.2 Deriving a prediction

3.2.1 Outline of the procedure

The steps required to achieve a prediction are as follows:

Step 1: Input data

The basic input data required for the procedure is given in Table 1. All other information required is derived from these basic data during the execution of the procedure.

TABLE 1

Basic input data

Parameter	Preferred resolution	Description
f	0.01	Frequency (GHz)
p	0.001	Required time percentage(s) for which the calculated basic transmission loss is not exceeded
φ_t, φ_r	0.001	Latitude of station (degrees)
ψ_t, ψ_r	0.001	Longitude of station (degrees)
h_{tg}, h_{rg}	1	Antenna centre height above ground level (m)
h_{ts}, h_{rs}	1	Antenna centre height above mean sea level (m)
G_t, G_r	0.1	Antenna gain in the direction of the horizon along the great-circle interference path (dBi)

NOTE 1 – For the interfering and interfered-with stations:

t: interferer

r: interfered-with station.

Step 2: Selecting average year or worst-month prediction

The choice of annual or "worst-month" predictions is generally dictated by the quality (i.e. performance and availability) objectives of the interfered-with radio system at the receiving end of the interference path. As interference is often a bidirectional problem, two such sets of quality objectives may need to be evaluated in order to determine the worst-case direction upon which the minimum permissible basic transmission loss needs to be based. In the majority of cases the quality objectives will be couched in terms of a percentage "of any month", and hence worst-month data will be needed.

The propagation prediction models predict the annual distribution of basic transmission loss. For average year predictions the percentages of time p, for which particular values of basic transmission loss are not exceeded, are used directly in the prediction procedure. If average worst-month predictions are required, the annual equivalent time percentage, p, of the worst-month time percentage, p_w, must be calculated for the path centre latitude φ using:

$$p = 10^{\left(\frac{\log(p_w) + \log(G_L) - 0.186\,\omega - 0.444}{0.816 + 0.078\,\omega} \right)} \quad \% \tag{1}$$

where:

ω: fraction of the path over water (see Table 3).

$$G_L = \begin{cases} \sqrt{1.1 + |\cos 2\varphi|^{0.7}} & \text{for } |\varphi| \le 45^\circ \\ \sqrt{1.1 - |\cos 2\varphi|^{0.7}} & \text{for } |\varphi| > 45^\circ \end{cases} \tag{1a}$$

If necessary the value of p must be limited such that $12\,p \ge p_w$.

Note that the latitude φ (degrees) is deemed to be positive in the Northern Hemisphere.

The calculated result will then represent the basic transmission loss for the required worst-month time percentage, p_w%.

Step 3: Radiometeorological data

The prediction procedure employs three radio-meteorological parameters to describe the variability of background and anomalous propagation conditions at the different locations around the world.

– ΔN (N-units/km), the average radio-refractive index lapse-rate through the lowest 1 km of the atmosphere, provides the data upon which the appropriate effective Earth radius can be calculated for path profile and diffraction obstacle analysis. Figures 11 and 12, respectively, provide world maps of average annual ΔN values and maximum monthly mean values for worst-month predictions. Note that ΔN is a positive quantity in this procedure.

– β_0 (%), the time percentage for which refractive index lapse-rates exceeding 100 N-units/km can be expected in the first 100 m of the lower atmosphere, is used to estimate the relative incidence of fully developed anomalous propagation at the latitude under consideration. The value of β_0 to be used is that appropriate to the path centre latitude.

– N_0 (N-units), the sea-level surface refractivity, is used only by the troposcatter model as a measure of location variability of the troposcatter scatter mechanism. Figure 13 provides annual values of N_0. As the scatter path calculation is based on a path geometry determined by annual or worst-month values of ΔN, there is no additional need for worst-month values of N_0. The correct values of ΔN and N_0 are given by the path-centre values as derived from the appropriate maps.

Point incidence of anomalous propagation, β_0 (%), for the path centre location is determined using:

$$\beta_0 = \begin{cases} 10^{-0.015|\varphi| + 1.67} \mu_1 \mu_4 & \% \quad \text{for } |\varphi| \le 70^\circ \\ 4.17 \mu_1 \mu_4 & \% \quad \text{for } |\varphi| > 70^\circ \end{cases} \tag{2}$$

where:

φ: path centre latitude (degrees).

The parameter μ_1 depends on the degree to which the path is over land (inland and/or coastal) and water, and is given by:

$$\mu_1 = \left[10^{\frac{-d_{tm}}{16 - 6.6\tau}} + \left[10^{-(0.496 + 0.354\tau)} \right]^5 \right]^{0.2} \tag{3}$$

where the value of μ_1 shall be limited to $\mu_1 \le 1$,

with:

$$\tau = \left[1 - e^{-\left(4.12 \times 10^{-4} \times d_{lm}^{2.41} \right)} \right] \tag{3a}$$

where:

d_{tm}: longest continuous land (inland + coastal) section of the great-circle path (km)

d_{lm}: longest continuous inland section of the great-circle path (km).

The radioclimatic zones to be used for the derivation of d_{tm} and d_{lm} are defined in Table 2.

$$\mu_4 = \begin{cases} 10^{(-0.935 + 0.0176|\varphi|)\log \mu_1} & \text{for } |\varphi| \le 70^\circ \\ 10^{0.3 \log \mu_1} & \text{for } |\varphi| > 70^\circ \end{cases} \tag{4}$$

TABLE 2

Radio-climatic zones

Zone type	Code	Definition
Coastal land	A1	Coastal land and shore areas, i.e. land adjacent to the sea up to an altitude of 100 m relative to mean sea or water level, but limited to a distance of 50 km from the nearest sea area. Where precise 100 m data are not available an approximate value, i.e. 300 ft, may be used
Inland	A2	All land, other than coastal and shore areas defined as "coastal land" above
Sea	B	Seas, oceans and other large bodies of water (i.e. covering a circle of at least 100 km in diameter)

Large bodies of inland water

A "large" body of inland water, to be considered as lying in Zone B, is defined as one having an area of at least 7 800 km^2, but excluding the area of rivers. Islands within such bodies of water are to be included as water within the calculation of this area if they have elevations lower than 100 m above the mean water level for more than 90% of their area. Islands that do not meet these criteria should be classified as land for the purposes of the water area calculation.

Large inland lake or wet-land areas

Large inland areas of greater than 7 800 km^2 which contain many small lakes or a river network should be declared as "coastal" Zone A1 by administrations if the area comprises more than 50% water, and more than 90% of the land is less than 100 m above the mean water level.

Climatic regions pertaining to Zone A1, large inland bodies of water and large inland lake and wetland regions, are difficult to determine unambiguously. Therefore administrations are invited to register with the ITU Radiocommunication Bureau (BR) those regions within their territorial boundaries that they wish identified as belonging to one of these categories. In the absence of registered information to the contrary, all land areas will be considered to pertain to climate Zone A2.

For maximum consistency of results between administrations it is strongly recommended that the calculations of this procedure be based on the ITU Digitized World Map (IDWM) which is available from the BR for mainframe or personal computer environments.

Effective Earth radius

The median effective Earth radius factor k_{50} for the path is determined using:

$$k_{50} = \frac{157}{157 - \Delta N} \tag{5}$$

Assuming a true Earth radius of 6 371 km, the median value of effective Earth radius a_e can be determined from:

$$a_e = 6\,371 \cdot k_{50} \quad \text{km} \tag{6}$$

Step 4: Path profile analysis

Values for a number of path-related parameters necessary for the calculations, as indicated in Table 3, must be derived via an initial analysis of the path profile based on the value of a_e given by equation (6). Information on the derivation, construction and analysis of the path profile is given in

Appendix 2. Having thus analysed the profile, the path will also have been classified into one of the three geometrical categories indicated in Table 4.

NOTE 1 – The determination of values for additional profile-related parameters required specifically for diffraction calculations is described in Recommendation ITU-R P.526.

Step 5: Calculation of propagation predictions

Table 4 indicates, for each type of path, the propagation models that are appropriate. The necessary equations for these individual propagation mechanism predictions are to be found in the text sections indicated in the Table. In order to build an overall prediction, the individual propagation mechanism predictions must be calculated and combined in the manner shown in § 4.7. For trans-horizon paths, elements from both the line-of-sight and diffraction models are reused within the combining process. Once this has been achieved for each of the required time percentages, the prediction is complete. It should be noted that equation (8c) used for the combination is a mathematical blend to prevent abrupt slope changes and not the linear addition of electrical powers.

TABLE 3

Parameter values to be derived from the path profile analysis

Path type	Parameter	Description
Trans-horizon	d	Great-circle path distance (km)
Trans-horizon	d_{lt}, d_{lr}	Distance from the transmit and receive antennas to their respective horizons (km)
Trans-horizon	θ_t, θ_r	Transmit and receive horizon elevation angles respectively (mrad)
Trans-horizon	θ	Path angular distance (mrad)
All	h_{ts}, h_{rs}	Antenna centre height above mean sea level (m)
Trans-horizon	h_{te}, h_{re}	Effective heights of antennas above the terrain (m) (see Appendix 2 for definitions)
All	d_b (1)	Aggregate length of the path sections over water (km)
All	ω (1)	Fraction of the total path over water: $\omega = d_b / d$ (7) where d is the great-circle distance (km) calculated using equation (37). For totally overland paths: $\omega = 0$
Trans-horizon	d_{ct} (1)	Distance over land from the first terminal (the interference source) to the coast along the great-circle interference path (km). For a terminal on a ship or sea platform d_{ct} is zero
Trans-horizon	d_{cr} (1)	Corresponding distance for the second (interfered-with) station (km)

(1) These parameters are only required when the path has one or more sections over water.
The exact values of d_{ct} and d_{cr} are only of importance if d_{ct} and $d_{cr} \leq 5$ km. If, in either or both cases, the distances are obviously in excess of 5 km, then it is only necessary to note the > 5 km condition. Few interference paths will in fact need detailed evaluation of these two parameters.

TABLE 4

Interference path classifications and propagation model requirements

Classification	Models required
Line-of-sight with first Fresnel zone clearance	Line-of-sight (§ 4.2) Clutter loss (§ 4.5, where appropriate)
Line-of-sight with sub-path diffraction, i.e. terrain incursion into the first Fresnel zone	Line-of-sight (§ 4.2) Diffraction (§ 4.3) Clutter loss (§ 4.3, where appropriate)
Trans-horizon	Diffraction (§ 4.3 for $d \leq 200$ km) Ducting/layer reflection (§ 4.5) Troposcatter (§ 4.4) Clutter loss (§ 4.6, where appropriate)

TABLE 5

Methods of deriving overall predictions

Path type	Action required
Line-of-sight	The prediction is obtained by summing the losses given by the line-of-sight and clutter loss models, i.e.: $L_b(p) = L_{b0}(p) + A_{ht} + A_{hr}$ dB (8a) where: $L_{b0}(p)$: predicted basic transmission loss not exceeded for p% of time given by the line-of-sight model A_{ht}, A_{hr}: appropriate additional losses due to height-gain effects in local clutter
Line-of-sight with sub-path diffraction	The prediction is obtained by summing the losses given by the line-of-sight and (sub-path) diffraction models and clutter models, i.e.: $L_b(p) = L_{b0}(p) + L_{ds}(p) + A_{ht} + A_{hr}$ dB (8b) where: $L_{ds}(p)$: prediction for p% of time given by the sub-path diffraction loss element of the diffraction model
Trans-horizon	The overall prediction is obtained in three stages: The unmodified ducting/layer reflection loss L_{ba} is obtained using the method in § 4.5. The modified ducting/layer reflection model loss, $L_{bam}(p)$, is found by application of the algorithm in § 4.7.1. The overall prediction can then be obtained by applying the following ancillary algorithm: $L_b(p) = -5 \log (10^{-0.2L_{bs}} + 10^{-0.2L_{bd}} + 10^{-0.2L_{bam}}) + A_{ht} + A_{hr}$ dB (8c) where $L_{bs}(p)$ and $L_{bd}(p)$: individual predicted basic transmission loss for p% of time given by the troposcatter and diffraction propagation models respectively. NOTE 1 – Where a model has not been proposed for a path (because the conditions given in Table 4 were not met), the appropriate term should be omitted from equation (8c).

4 Clear-air propagation models

4.1 General

The procedure given above invokes one or more separate propagation models to provide the components of the overall prediction. These propagation models are provided in this section.

4.2 Line-of-sight propagation (including short-term effects)

The basic transmission loss $L_{b0}(p)$ not exceeded for time percentage, p%, due to line-of-sight propagation is given by:

$$L_{b0}(p) = 92.5 + 20 \log f + 20 \log d + E_s(p) + A_g \quad \text{dB} \tag{9}$$

where:

$E_s(p)$: correction for multipath and focusing effects:

$$E_s(p) = 2.6 \left(1 - e^{-d/10}\right) \log (p / 50) \quad \text{dB} \tag{10}$$

A_g: total gaseous absorption (dB):

$$A_g = \left[\gamma_o + \gamma_w(\rho)\right] d \quad \text{dB} \tag{11}$$

where:

γ_o, $\gamma_w(\rho)$: specific attenuation due to dry air and water vapour, respectively, and are found from the equations in Recommendation ITU-R P.676

ρ: water vapour density:

$$\rho = 7.5 + 2.5\,\omega \quad \text{g/m}^3 \tag{11a}$$

ω: fraction of the total path over water.

4.3 Diffraction

The time variability of the excess loss due to the diffraction mechanism is assumed to be the result of changes in bulk atmospheric radio refractivity lapse rate, i.e. as the time percentage p reduces, the effective Earth radius factor $k(p)$ is assumed to increase. This process is considered valid for $\beta_0 \le p \le 50\%$. For time percentages less than β_0 signal levels are dominated by anomalous propagation mechanisms rather than by the bulk refractivity characteristics of the atmosphere. Thus for values of p less than β_0 the value of $k(p)$ has the value $k(\beta_0)$.

The value of effective Earth radius to use in diffraction calculations is given by:

$$a(p) = 6\,371 \cdot k(p) \quad \text{km} \tag{12}$$

where:

p: may take the values 50 or β_0

$k(50\%)$: is given by equation (5)

$k(\beta_0) =$ 3.

The excess diffraction loss $L_d(p)$ is computed by the method described in Recommendation ITU-R P.526, combined with a log-normal distribution of loss between 50% and β_0 as follows:

– for p = 50%, $L_d(50\%)$ is computed using the method described in Recommendation ITU-R P.526 for the median effective Earth radius a (50%);

– for $p \le \beta_0$, $L_d(\beta_0)$ is computed using the method described in Recommendation ITU-R P.526 for effective Earth radius $a(\beta_0)$, using the knife edges identified for the 50% (median) case;

– for $\beta_0 < p < 50\%$ $L_d(p)$ is given by:

$$L_d(p) = L_d(50\%) - F_i(p)\left[L_d(50\%) - L_d(\beta_0)\right] \quad (13)$$

where:

F_i: interpolation factor based on a log-normal distribution of diffraction loss over the range $\beta_0\% < p < 50\%$ given by:

$$F_i = I(p/100) / I(\beta_0/100) \quad (13a)$$

where $I(x)$ is the inverse cumulative normal function. A suitable approximation for $I(x)$ which may be used with confidence for $x < 0.5$ is given in Appendix 4.

NOTE 1 – Recommendation ITU-R P.526 can be used for the calculation of diffraction loss over either a line-of-sight path with sub-path obstruction, or a trans-horizon path.

The basic transmission loss not exceeded for p% time for a diffraction path is then given by:

$$L_{bd}(p) = 92.5 + 20 \log f + 20 \log d + L_d(p) + E_{sd}(p) + A_g \quad \text{dB} \quad (14)$$

where:

$E_{sd}(p)$: correction for multipath effects between the antennas and the horizon obstacles:

$$E_{sd}(p) = 2.6\left(1 - e^{-(d_{lt}+d_{lr})/10}\right) \log\left(\frac{p}{50}\right) \quad \text{dB} \quad (14a)$$

A_g: gaseous absorption determined using equations (11) and (11a).

4.4 Tropospheric scatter (Notes 1 and 2)

NOTE 1 – At time percentages much below 50%, it is difficult to separate the true tropospheric scatter mode from other secondary propagation phenomena which give rise to similar propagation effects. The "tropospheric scatter" model adopted in this Recommendation is therefore an empirical generalization of the concept of tropospheric scatter which also embraces these secondary propagation effects. This allows a continuous consistent prediction of basic transmission loss over the range of time percentages p from 0.001% to 50%, thus linking the ducting and layer reflection model at the small time percentages with the true "scatter mode" appropriate to the weak residual field exceeded for the largest time percentage.

NOTE 2 – This troposcatter prediction model has been derived for interference prediction purposes and is not appropriate for the calculation of propagation conditions above 50% of time affecting the performance aspects of trans-horizon radio-relay systems.

The basic transmission loss due to troposcatter, $L_{bs}(p)$ (dB) not exceeded for any time percentage, p, below 50%, is given by:

$$L_{bs}(p) = 190 + L_f + 20\log d + 0.573\theta - 0.15 N_0 + L_c + A_g - 10.1\left[-\log(p/50)\right]^{0.7} \quad \text{dB} \quad (15)$$

where:

L_f: frequency dependent loss:

$$L_f = 25 \log f - 2.5\left[\log(f/2)\right]^2 \quad \text{dB} \quad (15a)$$

L_c: aperture to medium coupling loss (dB):

$$L_c = 0.051 \cdot e^{0.055(G_t + G_r)} \quad \text{dB} \quad (15b)$$

N_0: path centre sea-level surface refractivity derived from Fig. 6

A_g: gaseous absorption derived from equation (11) using $\rho = 3$ g/m^3 for the whole path length.

4.5 Ducting/layer reflection

The prediction of the basic transmission loss, $L_{ba}(p)$ (dB) occurring during periods of anomalous propagation (ducting and layer reflection) is based on the following function:

$$L_{ba}(p) = A_f + A_d(p) + A_g \quad \text{dB} \tag{16}$$

where:

A_f: total of fixed coupling losses (except for local clutter losses) between the antennas and the anomalous propagation structure within the atmosphere:

$$A_f = 102.45 + 20 \log f + 20 \log (d_{lt} + d_{lr}) + A_{st} + A_{sr} + A_{ct} + A_{cr} \quad \text{dB} \tag{17}$$

A_{st}, A_{sr}: site-shielding diffraction losses for the interfering and interfered-with stations respectively:

$$A_{st,sr} = \begin{cases} 20\log\left[1 + 0.361\theta''_{t,r}\left(f \cdot d_{lt,lr}\right)^{1/2}\right] + 0.264\,\theta''_{t,r}\,f^{1/3} \text{ dB} & \text{for } \theta''_{t,r} > 0 \text{ mrad} \\ 0 \text{ dB} & \text{for } \theta''_{t,r} \le 0 \text{ mrad} \end{cases} \tag{18}$$

where:

$$\theta''_{t,r} = \theta_{t,r} - 0.1\,d_{lt,lr} \quad \text{mrad} \tag{18a}$$

A_{ct}, A_{cr}: over-sea surface duct coupling corrections for the interfering and interfered-with stations respectively:

$$A_{ct,cr} = -3\,e^{-0.25 d_{ct,cr}^2}\left[1 + \tanh\left(0.07(50 - h_{ts,rs})\right)\right] \quad \text{dB} \quad \text{for} \quad \omega \ge 0.75, \; d_{ct,cr} \le d_{lt,lr}, \; d_{ct,cr} \le 5 \text{ km} \tag{19}$$

$$A_{ct,cr} = 0 \quad \text{dB} \quad \text{for all other conditions} \tag{19a}$$

It is useful to note the limited set of conditions under which equation (19) is needed.

$A_d(p)$: time percentage and angular-distance dependent losses within the anomalous propagation mechanism:

$$A_d(p) = \gamma_d \cdot \theta' + A(p) \quad \text{dB} \tag{20}$$

where:

γ_d: specific attenuation:

$$\gamma_d = 5 \times 10^{-5}\, a_e\, f^{1/3} \quad \text{dB/mrad} \tag{21}$$

θ': angular distance (corrected where appropriate (via equation (22a)) to allow for the application of the site shielding model in equation (18)):

$$\theta' = \frac{10^3 d}{a_e} + \theta'_t + \theta'_r \quad \text{mrad} \tag{22}$$

$$\theta'_{t,r} = \begin{cases} \theta_{t,r} & \text{mrad} \quad \text{for } \theta_{t,r} \le 0.1 d_{lt,lr} \quad \text{mrad} \\ 0.1 d_{lt,lr} & \text{mrad} \quad \text{for } \theta_{t,r} > 0.1 d_{lt,lr} \quad \text{mrad} \end{cases} \tag{22a}$$

$A(p)$: time percentage variability (cumulative distribution):

$$A(p) = -12 + (1.2 + 3.7 \times 10^{-3} d) \log\left(\frac{p}{\beta}\right) + 12\left(\frac{p}{\beta}\right)^{\Gamma} \quad \text{dB} \tag{23}$$

$$\Gamma = \frac{1.076}{(2.0058 - \log\beta)^{1.012}} \times e^{-\left(9.51 - 4.8\log\beta + 0.198(\log\beta)^2\right) \times 10^{-6} \cdot d^{1.13}} \tag{23a}$$

$$\beta = \beta_0 \cdot \mu_2 \cdot \mu_3 \quad \% \tag{24}$$

μ_2: correction for path geometry:

$$\mu_2 = \left[\frac{500}{a_e} \frac{d^2}{\left(\sqrt{h_{te}} + \sqrt{h_{re}}\right)^2}\right]^{\alpha} \tag{25}$$

The value of μ_2 shall not exceed 1.

$$\alpha = -0.6 - \varepsilon \cdot 10^{-9} \cdot d^{3.1} \cdot \tau \tag{25a}$$

where:

ε = 3.5

τ: is defined in equation (3a)

and the value of α shall not be allowed to reduce below –3.4

μ_3: correction for terrain roughness:

$$\mu_3 = \begin{cases} 1 & \text{for } h_m \le 10 \text{ m} \\ \exp\left[-4.6 \times 10^{-5} (h_m - 10)(43 + 6 d_i)\right] & \text{for } h_m > 10 \text{ m} \end{cases} \tag{26}$$

$$d_i = \min(d - d_{lt} - d_{lr}, 40) \quad \text{km} \tag{26a}$$

A_g: total gaseous absorption determined from equations (11) and (11a).

The remaining terms have been defined in Tables 1 and 2 and Appendix 2.

4.6 Additional clutter losses

4.6.1 General

Considerable benefit, in terms of protection from interference, can be derived from the additional diffraction losses available to antennas which are imbedded in local ground clutter (buildings, vegetation etc.). This procedure allows for the addition of such clutter losses at either or both ends of the path in situations where the clutter scenario is known. Where there are doubts as to the certainty of the clutter environment this additional loss should not be included.

The clutter losses are designated as A_{ht} (dB) and A_{hr} (dB) for the interferer and interfered-with stations respectively. The additional protection available is height dependent, and is therefore modelled by a height-gain function normalized to the nominal height of the clutter. Appropriate nominal heights are available for a range of clutter types.

The correction applies to all clear-air predictions in this Recommendation, i.e. for all propagation modes and time percentages.

4.6.2 Clutter categories

Table 6 indicates the clutter (or ground cover) categories as defined in Recommendation ITU-R P.1058 for which the height-gain correction can be applied. The nominal clutter height, h_a (m) and distance from the antenna, d_k (km) are deemed to be "average" values most representative of the clutter type. However, the correction model has been made conservative in recognition of the uncertainties over the actual height that are appropriate in individual situations. Where the clutter parameters are more accurately known they can be directly substituted for the values taken from Table 6.

The nominal heights and distances given in Table 6 approximate to the characteristic height H_c and gap-width G_c defined in Recommendation ITU-R P.1058. However the model used here to estimate the additional losses due to shielding by clutter (ground cover) is intended to be conservative.

4.6.3 The height-gain model

The additional loss due to protection from local clutter is given by the expression:

$$A_h = 10.25 \times e^{-d_k} \left(1 - \tanh\left[6 \left(\frac{h}{h_a} - 0.625 \right) \right] \right) - 0.33 \quad \text{dB} \tag{27}$$

where:

d_k: distance (km) from nominal clutter point to the antenna (see Fig. 3)

h: antenna height (m) above local ground level

h_a: nominal clutter height (m) above local ground level.

TABLE 6

Nominal clutter heights and distances

Clutter (ground-cover) category	Nominal height, h_a (m)	Nominal distance, d_k (km)
High crop fields Park land Irregularly spaced sparse trees Orchard (regularly spaced) Sparse houses	4	0.1
Village centre	5	0.07
Deciduous trees (irregularly spaced) Deciduous trees (regularly spaced) Mixed tree forest	15	0.05
Coniferous trees (irregularly spaced) Coniferous trees (regularly spaced)	20	0.05
Tropical rain forest	20	0.03

TABLE 6 (*end*)

Clutter (ground-cover) category	Nominal height, h_a (m)	Nominal distance, d_k (km)
Suburban	9	0.025
Dense suburban	12	0.02
Urban	20	0.02
Dense urban	25	0.02
Industrial zone	20	0.05

Additional losses due to shielding by clutter (ground cover) should not be claimed for categories not appearing in Table 6.

FIGURE 3

Method of applying height-gain correction, A_{ht} or A_{hr}

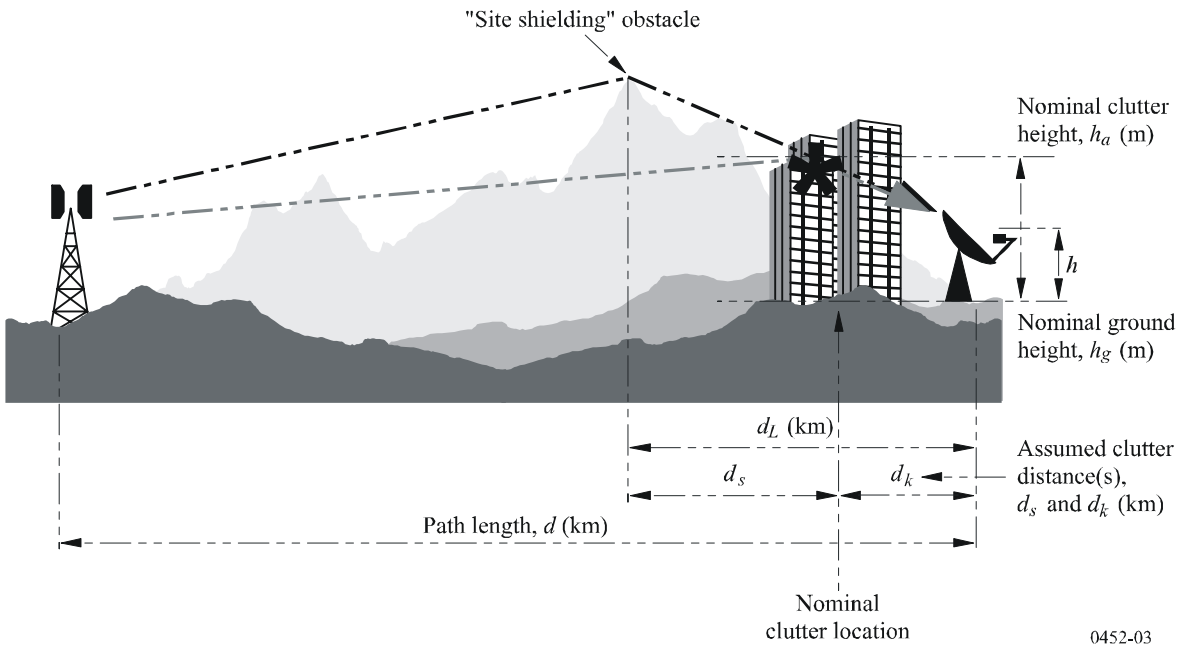

4.6.4 Method of application

The method of applying the height-gain correction, A_{ht} or A_{hr} (dB) is straightforward, and is shown in Fig. 3.

The steps to be added to the basic prediction procedure are as follows:

Step 1: where the clutter type is known or can be safely assumed, the main procedure is used to calculate the basic transmission loss to the nominal height, h_a, for the appropriate clutter type, as selected from Table 6. The path length to be used is $d - d_k$ (km). However where $d >> d_k$ this minor correction for d_k can safely be ignored.

Step 2: where there is a "site-shielding" obstacle that will provide protection to the terminal this should still be included in the basic calculation, but the shielding loss (A_{st} or A_{sr} (dB)) should be calculated to the height h_a at distance d_s, rather than to h at d_L as would otherwise be the case.

Step 3: once the main procedure is complete, the height gain correction from equation (27) can be added, as indicated in Table 5.

Step 4: where information on the clutter is not available, the basic calculation should be undertaken using distances d and d_L (if appropriate) and height h.

NOTE 1 – Clutter height-gain corrections should be added to both ends of the path where this is appropriate.

NOTE 2 – Where both the land height-gain correction and the sea duct coupling correction (A_{ct} or A_{cr} (dB)) are required (i.e. the antenna is close to the sea but there is intervening clutter), the two corrections can be used together as they are complementary and compatible.

NOTE 3 – If d is not significantly greater than d_k this model is not suitable.

4.7 The overall prediction

Table 5 gives the actions required to build the overall prediction for each classification of path type. For paths classified as line-of-sight or line-of-sight with sub-path diffraction, no further pre-processing of the individual model results are required before applying the required action from the Table.

4.7.1 Trans-horizon paths

In the case of trans-horizon paths, although the line-of-sight model is not a required model, use is made of the equivalent notional line-of-sight model loss in the combining process. The overall prediction is based upon calculation of a modified ducting/layer reflection loss, $L_{bam}(p)$, from the following function prior to the application of equation (8c) in Table 5:

$$L_{bam}(p) = L_{bda}(p) + (Lmin_{b0}(p) - L_{bda}(p)) \cdot F_j \tag{28}$$

where:

$$L_{bda}(p) = \begin{cases} L_{bd}(p) & \text{for} \quad Lmin_{ba}(p) > L_{bd}(p) \\ Lmin_{ba}(p) + (L_{bd}(p) - Lmin_{ba}(p)) \cdot F_k & \text{for} \quad Lmin_{ba}(p) \le L_{bd}(p) \end{cases} \tag{29}$$

$L_{bd}(p)$: diffraction loss evaluated at p% time from equation (14).

F_k: interpolation factor which blends the ducting/layer reflection into the diffraction loss with distance:

$$F_k = 1.0 - 0.5\left(1.0 + \tanh\left(3.0 \cdot \kappa \cdot \frac{(d - d_{sw})}{d_{sw}}\right)\right) \tag{30}$$

where:

d: great circle path length defined in Table 3

d_{sw}: fixed parameter determining the distance range of the transition; set to 20

κ: fixed parameter determining the approach slope at the ends of the range; set to 0.5

$Lmin_{ba}(p)$: modified ducting/layer reflection loss:

$$Lmin_{ba}(p) = \eta \cdot \ln\left(\exp\left(\frac{L_{ba}(p)}{\eta}\right) + \exp\left(\frac{L_{b0}(p)}{\eta}\right)\right) \tag{31}$$

where:

$L_{ba}(p)$: ducting/layer reflection loss from equation (16)

$L_{b0}(p)$: notional line-of-sight loss for the path evaluated from equation (9)

η = 2.5

$Lmin_{b0}(p)$: notional minimum propagation loss that the modified ducting/layer reflection loss can attain:

$$Lmin_{b0}(p) = \begin{cases} L_{b0}(p) & \text{for } p < \beta_0 \\ L_{bd50} - (L_{bd50} - L_{b0\beta}) \cdot F_i & \text{for } p \geq \beta_0 \end{cases} \quad (32)$$

where:

$L_{b0\beta}$: notional line-of-sight loss evaluated at β_0% time from equation (9):

$$L_{b0\beta} = L_{b0}(\beta_0 \%) \quad (33)$$

L_{bd50}: diffraction loss evaluated at 50% time from equation (14):

$$L_{bd50} = L_{bd}(50\%) \quad (34)$$

F_i: interpolation factor based on a log-normal distribution of diffraction loss defined in equation (13a)

F_j: interpolation factor which blends the modified ducting/layer reflection into the notional line-of-sight loss:

$$F_j = 1.0 - 0.5\left(1.0 + \tanh\left(3.0 \cdot \xi \cdot \frac{(\theta - \Theta)}{\Theta}\right)\right) \quad (35)$$

where:

Θ = 0.3

ξ = 0.8

θ: path angular distance defined in Table 7.

4.8 Calculation of transmission loss

The method described in § 4.2 to 4.7 above provides the basic transmission loss between the two stations. In order to calculate the signal level at one station due to interference from the other it is necessary to know the transmission loss, which takes account of the antenna gains of the two stations in the direction of the radio (i.e. interference) path between them.

The following procedure provides a method for the calculation of transmission loss between two terrestrial stations. As intermediate steps in the method, it also provides formulae for the calculation of the great-circle path length and angular distance based on the stations' geographic coordinates, as opposed to the derivations of these quantities from the path profile, as assumed in Table 3.

Calculate the angle subtended by the path at the centre of the Earth, δ, from the stations' geographic coordinates using:

$$\delta = \arccos(\sin(\varphi_t)\sin(\varphi_r) + \cos(\varphi_t)\cos(\varphi_r)\cos(\psi_t - \psi_r)) \quad \text{rad} \quad (36)$$

The great circle distance, d, between the stations is:

$$d = 6\,371 \cdot \delta \quad \text{km} \quad (37)$$

Calculate the bearing (azimuthal direction clockwise from true North) from station t to station r using:

$$\alpha_{tr} = \arccos(\{\sin(\varphi_r) - \sin(\varphi_t)\cos(\delta)\}/\sin(\delta)\cos(\varphi_t)) \quad \text{rad} \quad (38)$$

Having implemented (38), if $\psi_t - \psi_r > 0$ then:

$$\alpha_{tr} = 2\pi - \alpha_{tr} \quad \text{rad} \quad (39)$$

Calculate the bearing from station r to station t, α_{rt}, by symmetry from equations (38) and (39).

Next, assume that the main beam (boresight) direction of station t is (ε_t, α_t) in (elevation, bearing), while the main beam direction of station r is (ε_r, α_r). To obtain the elevation angles of the radio (i.e. interference) path at stations t and r, ε_{pt} and ε_{pr}, respectively, it is necessary to distinguish between line-of-sight and trans-horizon paths. For example, for line-of-sight paths:

$$\varepsilon_{pt} = \frac{h_r - h_t}{d} - \frac{d}{2a_e} \quad \text{rad} \tag{40a}$$

and

$$\varepsilon_{pr} = \frac{h_t - h_r}{d} - \frac{d}{2a_e} \quad \text{rad} \tag{40b}$$

where h_t and h_r are the heights of the stations above mean sea level (km), while for trans-horizon paths, the elevation angles are given by their respective horizon angles:

$$\varepsilon_{pt} = \frac{\theta_t}{1\,000} \quad \text{rad} \tag{41a}$$

and

$$\varepsilon_{pr} = \frac{\theta_r}{1\,000} \quad \text{rad} \tag{41b}$$

Note that the radio horizon angles, θ_t and θ_r (mrad), are first introduced in Table 3 and are defined in § 5.1.1 and 5.1.3, respectively, of Appendix 1 to Annex 1.

To calculate the off-boresight angles for stations t and r, χ_t and χ_r, respectively, in the direction of the interference path at stations t and r, it is recommended to use:

$$\chi_t = \arccos(\cos(\varepsilon_t)\cos(\varepsilon_{pt})\cos(\alpha_{tr} - \alpha_t) + \sin(\varepsilon_t)\sin(\varepsilon_{pt})) \tag{42a}$$

and

$$\chi_r = \arccos(\cos(\varepsilon_r)\cos(\varepsilon_{pr})\cos(\alpha_{rt} - \alpha_r) + \sin(\varepsilon_r)\sin(\varepsilon_{pr})) \tag{42b}$$

Using their respective off-boresight angles, obtain the antenna gains for stations t and r, G_t and G_r, respectively (dB). If the actual antenna radiation patterns are not available, the variation of gain with off-boresight angle may be obtained from the information in Recommendation ITU-R S.465.

To obtain the transmission loss, L, use:

$$L = L_b(p) - G_t - G_r \quad \text{dB} \tag{43}$$

For clear-air interference scenarios where radio propagation is dominated by troposcatter, the elevation angles will be slightly greater than the radio horizon angles, θ_t and θ_r. The use of these should introduce negligible error, unless these also coincide with their respective stations' boresight directions.

5 Hydrometeor-scatter interference prediction

In contrast to the preceding clear-air prediction methods described above, the hydrometeor-scatter interference prediction methodology described below develops expressions for the transmission loss between two stations directly, since it requires a knowledge of the interfering and victim antenna radiation patterns for each station.

The method is quite general, in that it can be used with any antenna radiation pattern which provides a method for determining the antenna gain at any off-boresight axis angle. Radiation patterns such as those in Recommendations ITU-R P.620, ITU-R F.699, ITU-R F.1245, ITU-R S.465 and ITU-R S.580, for example, can all be used, as can more complex patterns based Bessel functions and actual measured patterns if these are available. The method can also be used with omnidirectional or sectoral antennas, such as those characterized in Recommendation ITU-R F.1336, the gain of which is generally determined from the vertical off-boresight axis angle (i.e. the elevation relative to the angle of maximum gain).

The method is also general in that it is not restricted to any particular geometry, provided that antenna radiation patterns are available with ±180° coverage. Thus, it includes both main beam-to-main beam coupling and side lobe-to-main beam coupling, and both great-circle scatter and side-scatter geometries. The method can compute interference levels for both long-path (> 100 km) and short-path geometries (down to a few kilometres) with arbitrary elevation and azimuthal angles at either station. The methodology is therefore appropriate to a wide range of scenarios and services, including the determination of rain-scatter interference between two terrestrial stations, between a terrestrial station and an earth station, and between two earth stations operating in bidirectionally allocated frequency bands.

An implementation of the model is available from the Bureau in Fortran, using the antenna radiation patterns in Recommendations ITU-R P.620, ITU-R F.1245 and ITU-R F.1336.

5.1 Introduction

The methodology is based on application of the bistatic radar equation, which can be written in terms of the power P_r received at a receiving station from scattering by rain of the power P_t transmitted by a transmitting station:

$$P_r = P_t \frac{\lambda^2}{(4\pi)^3} \iiint_{all\ space} \frac{G_t G_r \eta A}{r_t^2 r_r^2} \mathrm{d}V \quad \text{W} \tag{44}$$

where:

λ: wavelength

G_t: gain (linear) of the transmitting antenna

G_r: gain (linear) of the receiving antenna

η: scattering cross-section per unit volume, δV (m^2/m^3)

A: attenuation along the path from transmitter to receiver (in linear terms)

r_t: distance from the transmitter to the scattering volume element

r_r: distance from the scattering volume element to the receiver.

Expressed in terms of the transmission loss, (dB), for scattering between two stations, Station 1 and Station 2, the bistatic radar equation becomes:

$$L = 208 - 20 \log f - 10 \log Z_R - 10 \log C + 10 \log S + A_g - M \quad \text{dB} \tag{45}$$

where:

f: frequency (GHz)

Z_R: radar reflectivity at ground level, which can be expressed in terms of the rainfall rate, R (mm/h):

$$Z_R = 400 R^{1.4} \tag{46}$$

$10 \log S$: correction (dB), to account for the deviation from Rayleigh scattering at frequencies above 10 GHz:

$$10\log S = \begin{cases} R^{0.4} \cdot 10^{-3}\left[4(f-10)^{1.6}\left(\frac{1+\cos\varphi_S}{2}\right)+5(f-10)^{1.7}\left(\frac{1-\cos\varphi_S}{2}\right)\right] & \text{for } f > 10\,\text{GHz} \\ 0 & \text{for } f \le 10\,\text{GHz} \end{cases} \quad (47)$$

where:

φ_S: scattering angle

A_g: attenuation due to atmospheric gases along the path from transmitter to receiver (dB), calculated from Recommendation ITU-R P.676 Annex 2.

M: any polarization mismatch between transmitting and receiving systems (dB).

In the model given here, scattering is confined to that within a rain cell, which is defined as being of circular cross-section, with a diameter depending on the rainfall rate:

$$d_c = 3.3R^{-0.08} \quad \text{km} \quad (48)$$

Within the rain cell, the rainfall rate, and hence the radar reflectivity, is assumed to be constant up to the rain height, h_R. Above the rain height, the reflectivity is assumed to decrease linearly with height at a rate of –6.5 dB/km.

The scatter transfer function, C, is then the volume integral over the rain cell and can be written, in cylindrical coordinates, as:

$$C = \int_0^{h_{max}} \int_0^{2\pi} \int_0^{\frac{d_c}{2}} \frac{G_1 G_2}{r_1^2 r_2^2} A\zeta \cdot r \, dr d\varphi dh \quad (49)$$

where:

G_1, G_2: linear gains of Station 1 and Station 2, respectively

r_1, r_2: distances (km) from the integration element δV to Station 1 and Station 2, respectively

A: attenuation due to rain, both inside and outside the rain cell, expressed in linear terms

ζ: height dependence of the radar reflectivity:

$$\zeta = \begin{cases} 1 & \text{for } h \le h_R \\ 10^{-0.65(h-h_R)} & \text{for } h > h_R \end{cases} \quad (50)$$

h_R: rain height (km)

r, φ, h: variables of integration within the rain cell.

The integration is carried out numerically, in cylindrical coordinates. However, it is convenient initially to consider the geometry of the scattering from the transmitting station through a rain cell to the receiving station in terms of a Cartesian coordinate system with Station 1 taken as the origin, since the actual position of the rain cell will not immediately be defined, especially in the case of side scattering.

Within the Cartesian coordinate reference, it is advantageous, in terms of simplicity, first to convert the various geometrical parameters from their actual curved-Earth values to a plane-Earth representation.

The existence of main beam-to-main beam coupling between the antennas is established from the geometry, and the rain cell is then located at the point of intersection between the main beam axes. If main beam-to-main beam coupling does not exist, then the rain cell is located along the main beam axis of Station 1, centred at the point of closest approach to the main beam axis of Station 2. In this case, the transmission losses should be determined for a second case with the parameters of each station interchanged, and the worst-case loss distribution taken as representative of the likely interference levels.

5.2 Input parameters

Table 7 lists all the input parameters which are required for implementation of the method to calculate the cumulative distribution of transmission loss between two stations due to rain scatter.

TABLE 7

List of input parameters

(Suffix 1 refers to parameters for Station 1, suffix 2 refers to parameters for Station 2)

Parameter	Units	Description
d	km	Distance between stations
f	GHz	Frequency
h_{1_loc}, h_{2_loc}	km	Local heights above mean sea level of Station 1, Station 2
$G_{max\text{-}1}$, $G_{max\text{-}2}$	dB	Maximum gains for each antenna
$h_R(p_h)$	km	Cumulative distribution of rain height exceeded as a function of percentage of time p_h (see Note 1)
M	dB	Polarization mismatch between systems
P	hPa	Surface pressure (default 1013.25 hPa)
$R(p_R)$	mm/h	Cumulative distribution of rainfall rate exceeded as a function of percentage of time p_R
T	°C	Surface temperature (default 15° C)
α_{1_loc}, α_{2_loc}	rad	Local bearings of Station 1 from Station 2, and Station 2 from Station 1, in the clockwise sense
ε_{H1_loc}, ε_{H2_loc}	rad	Local horizon angles for Station 1 and Station 2
ρ	g/m^3	Surface water-vapour density (default 8 g/m^3)
τ	degrees	Polarization angle of link (0° for horizontal polarization, 90° for vertical polarization)

NOTE 1 – If the distribution is not available, use the median rain height, h_R, together with Table 8.

5.3 The step-by-step procedure

Step 1: Determination of meteorological parameters

In order to derive the cumulative distribution of transmission loss due to rain scatter in terms of the percentage of time such losses are exceeded, the input parameters required are the probability distributions of rainfall rate and rain height. If local values for these are available, then these should be used. In the absence of local values, Recommendation ITU-R P.837 can be used to obtain the cumulative distributions of rainfall rate for any location, while the median rain height can be obtained from Recommendation ITU-R P.839. As a default for the cumulative distribution of rain heights, the distribution of rain height relative to the median value in Table 8 can be used.

TABLE 8

Cumulative distribution of rain height relative to its median value

Rain height difference (km)	Probability of exceedance (%)
−1.625	100.0
−1.375	99.1
−1.125	96.9
−0.875	91.0
−0.625	80.0
−0.375	68.5
−0.125	56.5
0.125	44.2
0.375	33.5
0.625	24.0
0.875	16.3
1.125	10.2
1.375	6.1
1.625	3.4
1.875	1.8
2.125	0.9
2.375	0.0

The cumulative distributions of both rainfall rate and rain height are converted into probability density functions in the following way. For each interval between two adjacent values of rainfall-rate or rain-height, the mean value is taken as being representative for that interval, and its probability of occurrence is the difference between the two corresponding exceedance probabilities. Any values for which h_R is less than 0 km when using Table 7 are set to 0 km with their probabilities being added together.

It is assumed that rainfall rate and rain height are statistically independent of each other, so that the probability of occurrence for any given pair of rainfall-rate/rain-height combinations is simply the product of the individual probabilities.

For each pair of rainfall-rate/rain-height values, the transmission loss is calculated according to the following steps.

Step 2: Conversion of geometrical parameters to plane-Earth representation

The geometry of rain scattering between two stations is determined from the basic input parameters of the great-circle distance d between the two stations, the local values for the elevation angles of each station antenna, $\varepsilon_{1\text{-}loc}$ and $\varepsilon_{2\text{-}loc}$, and azimuthal offsets of the antenna main-beam axes for each station from the direction of the other station defined as positive in the clockwise sense, $\alpha_{1\text{-}loc}$ and $\alpha_{2\text{-}loc}$. Station 1 is taken as the reference position, i.e. the origin, for the Cartesian coordinate system, and the reference parameters are thus:

$$\varepsilon_1 = \varepsilon_{1\_loc},\ \alpha_1 = \alpha_{1\_loc} \quad \text{and:}\ \varepsilon_{H1} = \varepsilon_{H1\_loc} \quad \text{rad} \tag{51}$$

First convert all the geometrical parameters to a common Cartesian coordinate system, taking Station 1 as the origin, with the horizontal plane as the *x*-*y* plane, the *x*-axis pointing in the direction of Station 2 and the *z*-axis pointing vertically upwards. Figure 4 illustrates the geometry on the curved Earth (for the simplified case of forward scattering, i.e. along the great circle), where r_{eff} is the effective radius of the Earth,

$$r_{eff} = k_{50} R_E \quad \text{km} \tag{52}$$

where:

k_{50}: median effective Earth radius factor = 1.33

R_E: true Earth radius = 6 371 km.

The two stations are separated by the great-circle distance d (km), subtending an angle δ at the Earth's centre:

$$\delta = \frac{d}{r_{eff}} \quad \text{rad} \tag{53}$$

The local vertical at Station 2 is tilted by the angle δ from the local vertical at Station 2, i.e. the *Z*-axis. The elevation and azimuthal angles of Station 2 are thus converted to the plane-Earth representation as follows, where the subscript *loc* refers to the local values.

FIGURE 4

Geometry of stations on curved Earth

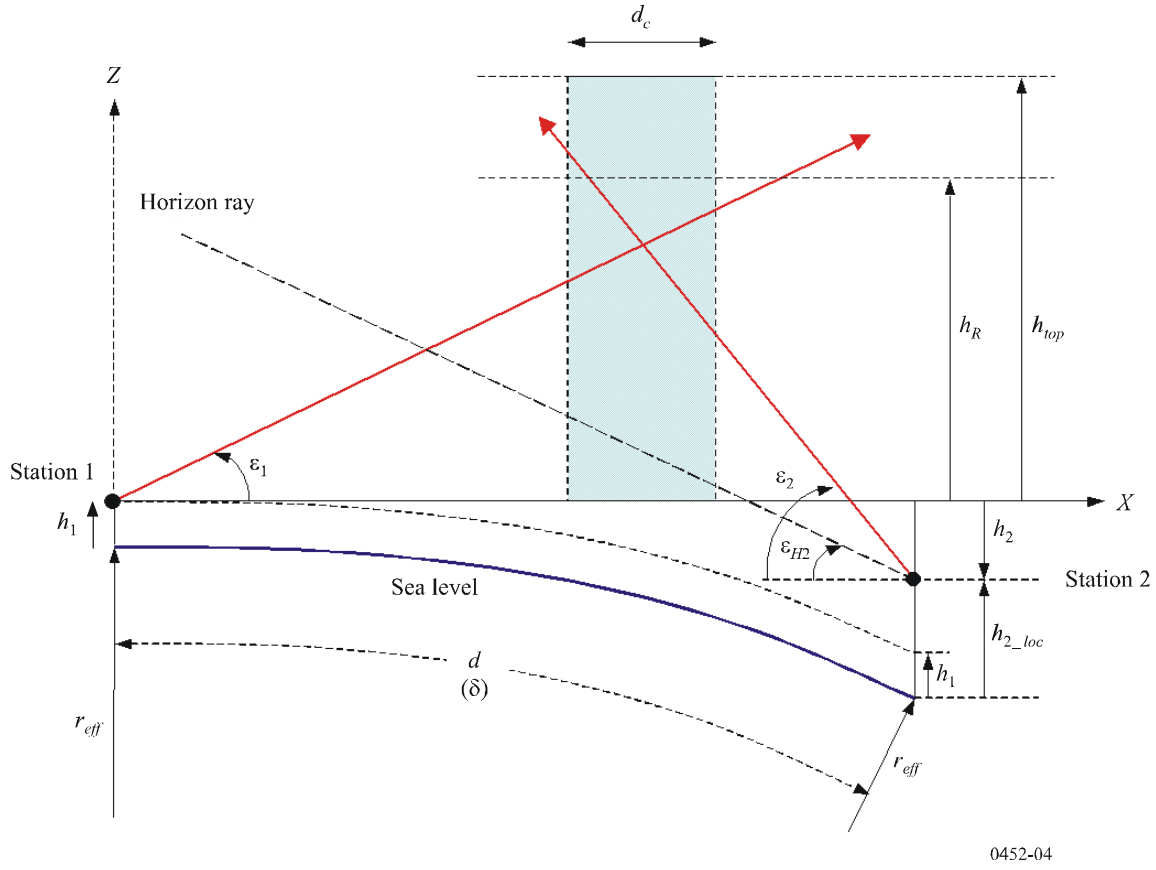

Calculate the elevation angle of Station 2:

$$\varepsilon_2 = \arcsin\left(\cos\varepsilon_{2\_loc}\cos\alpha_{2\_loc}\sin\delta + \sin\varepsilon_{2\_loc}\cos\delta\right) \tag{54}$$

and the horizon angle at Station 2:

$$\varepsilon_{H2} = \arcsin\left(\cos\varepsilon_{H2\_loc}\cos\alpha_{2\_loc}\sin\delta + \sin\varepsilon_{H2\_loc}\cos\delta\right) \tag{55}$$

The azimuthal offset of Station 2 from Station 1 is:

$$\alpha_2 = \arctan\left(\frac{\cos\varepsilon_{2\_loc}\sin\alpha_{2\_loc}}{\cos\varepsilon_{2\_loc}\cos\alpha_{2\_loc}\cos\delta - \sin\varepsilon_{2\_loc}\sin\delta}\right) \tag{56}$$

and the height of Station 2 above the reference plane is given by:

$$h_2 = h_{2\_loc} - h_1 - d\frac{\delta}{2} \qquad \text{km} \tag{57}$$

The azimuthal separation between the two stations at the point of intersection between ground-plane projections of the main-beam axes is:

$$\alpha_S = \pi - (\alpha_1 - \alpha_2) \qquad \text{rad} \tag{58}$$

Step 3: Determination of link geometry

The method for determining the geometry of the scatter links uses vector notation, in which a vector in three-dimensional space is represented by a three-element single-column matrix comprising the lengths of the projections of the line concerned onto the Cartesian *x*, *y* and *z* axes. A vector will be represented by a symbol in bold typeface. Thus, a vector assignment may, in general, be written:

$$\mathbf{V} = \begin{bmatrix} x \\ y \\ z \end{bmatrix}$$

A unit-length vector will, in general, be represented by the symbol **V**, while a general vector (i.e. including magnitude) will be represented by another, appropriate symbol, for example **R**.

The basic geometry for rain scattering is illustrated schematically in Fig. 5 for the general case of side scattering, where the two main-beam axes do not, in fact, intersect. In other words, this example represents side-lobe to main-lobe coupling. The interference path may be from the Station 2 side-lobes into the Station 1 main beam, or vice versa.

FIGURE 5

Schematic of rain scatter geometry for the general case of side scattering

(Note that the antenna beams do not coincide in this example,
and the "squint angle" is non-zero – see equations (60) and (61))

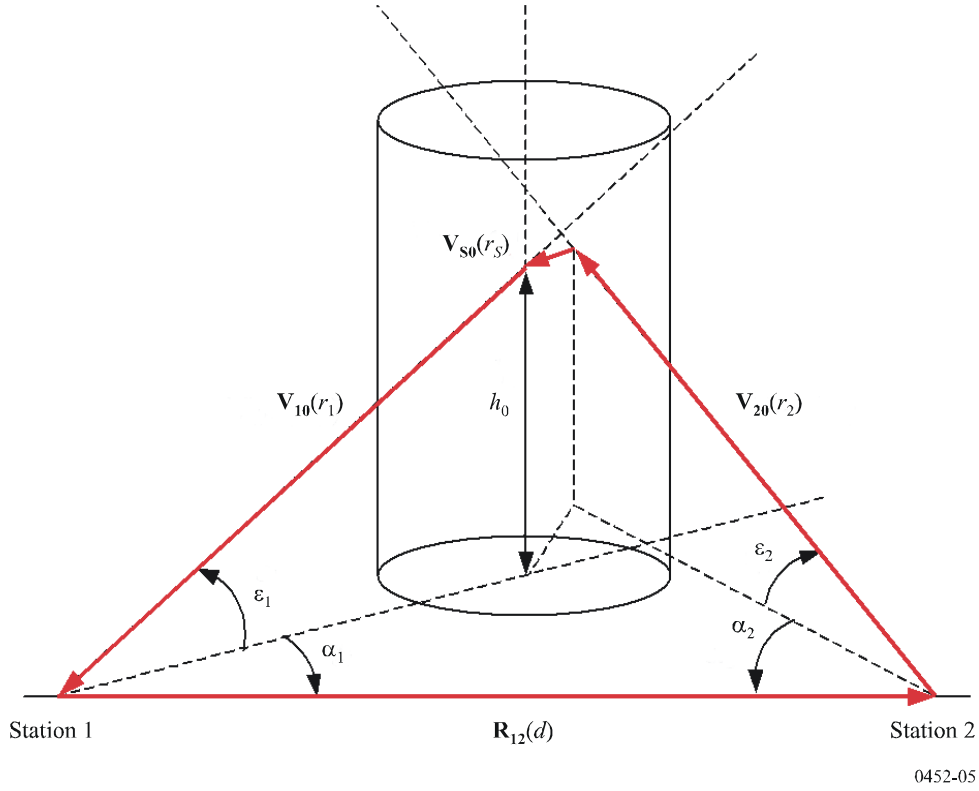

The centre of the rain cell is located along the main beam antenna axis of Station 1 at the point of closest approach between the two antenna beams. The geometry is established in vector notation as follows.

The vector from Station 1 to Station 2 is defined as:

$$\mathbf{R_{12}} = \begin{bmatrix} d \\ 0 \\ h_2 \end{bmatrix} \quad \text{km} \tag{59}$$

The vectors $\mathbf{R_{12}}$, $r_2\mathbf{V_{20}}$, $r_S\mathbf{V_{S0}}$ and $r_1\mathbf{V_{10}}$ form a closed three-dimensional polygon, with the vector $\mathbf{V_{S0}}$ perpendicular to both $\mathbf{V_{10}}$ and $\mathbf{V_{20}}$. In the example illustrated in Fig. 5, the vector $\mathbf{V_{S0}}$ is directed out of the page.

Taking the curvature of the Earth into account, calculate the unit-length vector $\mathbf{V_{10}}$ in the direction of the Station 1 antenna main beam:

$$\mathbf{V_{10}} = \begin{bmatrix} \cos\varepsilon_1 \cos\alpha_1 \\ -\cos\varepsilon_1 \sin\alpha_1 \\ \sin\varepsilon_1 \end{bmatrix} \tag{60}$$

and the unit-length vector $\mathbf{V_{20}}$ in the direction of the Station 2 antenna main beam:

$$\mathbf{V_{20}} = \begin{bmatrix} \sin\varepsilon_{2\_loc}\sin\delta - \cos\varepsilon_{2\_loc}\cos\alpha_{2\_loc}\cos\delta \\ \cos\varepsilon_{2\_loc}\sin\alpha_{2\_loc} \\ \sin\varepsilon_{2\_loc}\cos\delta + \cos\varepsilon_{2\_loc}\cos\alpha_{2\_loc}\sin\delta \end{bmatrix} \tag{61}$$

The method now uses the scalar product of two vectors, which is written and evaluated as:

$$\mathbf{V_1} \cdot \mathbf{V_2} = x_1 x_2 + y_1 y_2 + z_1 z_2 \qquad \text{where } \mathbf{V_1} = \begin{bmatrix} x_1 \\ y_1 \\ z_1 \end{bmatrix}$$

The scattering angle φ_S, i.e. the angle between the two antenna beams, is determined from the scalar product of the two vectors $\mathbf{V_{10}}$ and $\mathbf{V_{20}}$:

$$\varphi_S = \arccos\left(-\mathbf{V_{20}} \cdot \mathbf{V_{10}}\right) \tag{62}$$

If $\varphi_S < 0.001$ rad, then the two antenna beams are approximately parallel, and it can be assumed that any coupling by rain scatter will be negligible.

As indicated in Fig. 5, the four vectors $\mathbf{R_{12}}$, $r_2\mathbf{V_{20}}$, $r_S\mathbf{V_{S0}}$ and $r_1\mathbf{V_{10}}$ form a closed three-dimensional polygon, i.e.:

$$\mathbf{R_{12}} + r_2\mathbf{V_{20}} + r_S\mathbf{V_{S0}} - r_1\mathbf{V_{10}} = 0 \tag{63}$$

and this can be solved for the distances r_i. The method uses the vector product of two vectors, which is written and evaluated as follows. The vector (or cross) product is:

$$\mathbf{V_1} \times \mathbf{V_2} = \begin{bmatrix} y_1 z_2 - z_1 y_2 \\ z_1 x_2 - x_1 z_2 \\ x_1 y_2 - y_1 x_2 \end{bmatrix}$$

The unit-length vector $\mathbf{V_{S0}}$, which is perpendicular to both antenna beams, is calculated from the vector product $\mathbf{V_{20}} \times \mathbf{V_{10}}$:

$$\mathbf{V_{S0}} = \frac{\mathbf{V_{20}} \times \mathbf{V_{10}}}{\sin\varphi_S} \tag{64}$$

Equation (63) can now be solved using the determinant of three vectors, which is written and evaluated thus:

$$\det[\mathbf{V_1} \quad \mathbf{V_2} \quad \mathbf{V_3}] = \det\begin{bmatrix} x_1 & x_2 & x_3 \\ y_1 & y_2 & y_3 \\ z_1 & z_2 & z_3 \end{bmatrix} = x_1(y_2 z_3 - y_3 z_2) + x_2(y_3 z_1 - y_1 z_3) + x_3(y_1 z_2 - y_2 z_1)$$

Calculate the distance between the two beams at their closest approach:

$$r_S = \frac{\det[\mathbf{V_{10}} \quad \mathbf{V_{20}} \quad \mathbf{V_{12}}]}{\det[\mathbf{V_{10}} \quad \mathbf{V_{20}} \quad \mathbf{V_{S0}}]} \tag{65}$$

The slant-path distance r_1 from Station 1 along its main beam to the point of closest approach to the Station 2 main beam is:

$$r_1 = \frac{\det[\mathbf{V_{12}} \quad \mathbf{V_{20}} \quad \mathbf{V_{S0}}]}{\det[\mathbf{V_{10}} \quad \mathbf{V_{20}} \quad \mathbf{V_{S0}}]} \tag{66}$$

while the corresponding slant-path distance r_2 from Station 2 along its main beam to the point of closest approach to the Station 1 main beam (noting the unary minus) is:

$$r_2 = \frac{-\det[\mathbf{V_{10}} \quad \mathbf{V_{12}} \quad \mathbf{V_{S0}}]}{\det[\mathbf{V_{10}} \quad \mathbf{V_{20}} \quad \mathbf{V_{S0}}]} \tag{67}$$

Calculate the off-axis squint angle ψ_1 at Station 1 of the point of closest approach on the Station 2 main beam axis:

$$\Psi_1 = \arctan\left(\frac{|r_S|}{r_1}\right) \tag{68}$$

and the corresponding off-axis squint angle at Station 1 of the point of closest approach on the Station 1 main beam axis:

$$\Psi_2 = \arctan\left(\frac{|r_S|}{r_2}\right) \tag{69}$$

From these parameters, determine whether or not there is main beam-to-main beam coupling between the two stations. For there to be main beam-to-main beam coupling, the squint angle should be less than the 3 dB beamwidth of the relevant antenna. For squint angles greater than this, there will effectively be little or no main beam-to-main beam coupling, and the transmission path will be influenced predominantly by side-lobe-to-main beam coupling. If this be the case, two possibilities should be investigated, with the centre of the rain cell located along the main-beam axis of each antenna in turn, and the lowest transmission loss taken to represent the worst-case situation. Since the default location of the rain cell is at the point of closest approach along the main-beam axis of Station 1, this can easily be accomplished by substituting the parameters of Station 2 for those of Station 1, and vice versa.

Finally, it is necessary also to determine the horizontal projections of the various distances calculated above, from which the location of the rain cell can be established. Figure 6 shows a plan view for the general case of side scattering.

FIGURE 6

Plan view of geometry for side scattering

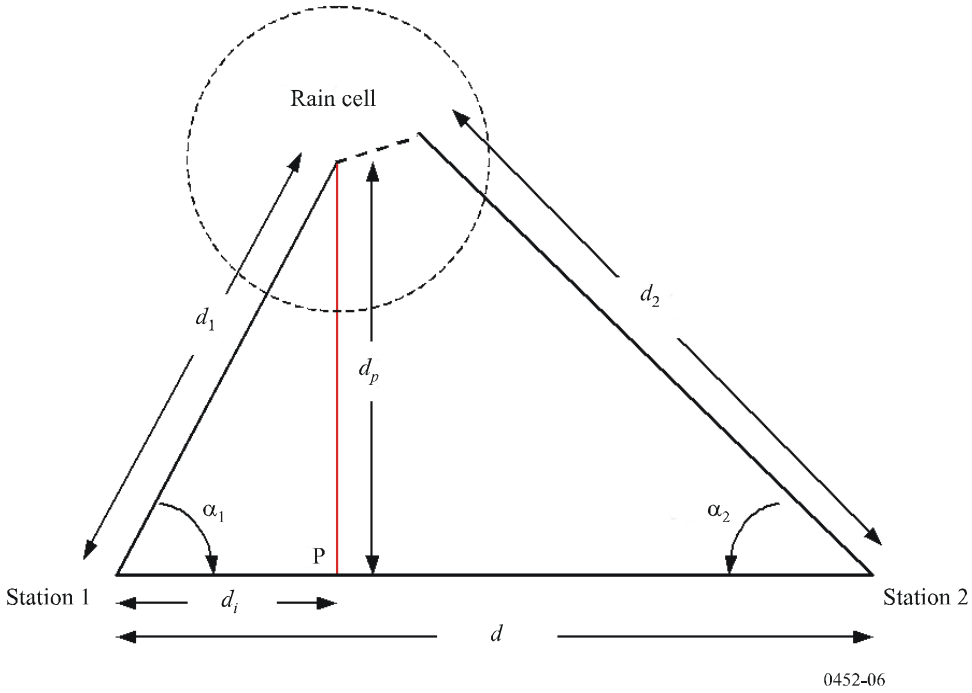

Calculate the horizontal distance from Station 1 to the centre of the rain cell, defined as that point on the ground immediately below the point of closest approach on the Station 1 main-beam axis:

$$d_1 = r_1 \cos\varepsilon_1 \quad \text{km} \tag{70}$$

and the corresponding horizontal distance from Station 2 to the ground-plane projection of its point of closest approach:

$$d_2 = r_2 \cos\varepsilon_2 \quad \text{km} \tag{71}$$

The height above the ground of the point of closest approach on the Station 1 main-beam axis is:

$$h_0 = |r_1| \sin\varepsilon_1 \quad \text{km} \tag{72}$$

while, for cases where there is no main beam-to-main beam coupling, the height of the point of closest approach on the Station 2 main-beam axis is:

$$h_{2\_0} = |r_2| \sin\varepsilon_2 \quad \text{km} \tag{73}$$

The height parameters associated with the rain cell need to be corrected for any offset from the great-circle path in the case of side scattering. The distance from the great-circle path between the two stations is:

$$d_p = d_1 \sin\alpha_1 \tag{74}$$

and the angular separation is then:

$$\delta_p = \frac{d_p}{r_{eff}} \quad \text{km} \tag{75}$$

Now determine the correction for side scattering:

$$h_c = h_1 + d_p \frac{\delta_p}{2} \quad \text{km} \tag{76}$$

Note that this correction is also be applied to other parameters associated with the rain cell, i.e. the rain height, h_R and the upper limit for integration, h_{top}, and in the determination of gaseous attenuation (see Step 8), which requires the use of local parameters.

This now establishes the main static geometrical parameters for locating the rain cell with respect to the stations and for evaluating the transmission loss due to rain scatter. It is necessary now to consider the geometry for the integration element, which can be anywhere within the rain cell, up to a predetermined upper limit for the integration, h_{top}, in order to determine the antenna gains at each point within the rain cell and the path attenuations within the rain cell in the directions of each station. To do this, the coordinate system is changed to cylindrical coordinates (r, φ, h), centred on the rain cell.

Step 4: Determination of geometry for antenna gains

In order to calculate the gain of each antenna at the integration element at coordinates (r, φ, h) using such an antenna radiation pattern, and the path attenuation within the rain cell, it is necessary to calculate the off-axis boresight angle at the position of the integration element and the path lengths from the integration element to the edge of the rain cell in the directions of each station. Figure 7 illustrates the geometry, where point A represents an arbitrary integration element at coordinates (r, φ, h), and point B is the projection of this point on the ground plane. A plan view of the geometry is shown in Fig. 8.

FIGURE 7

Geometry for determination of antenna gains and path attenuation within the rain cell

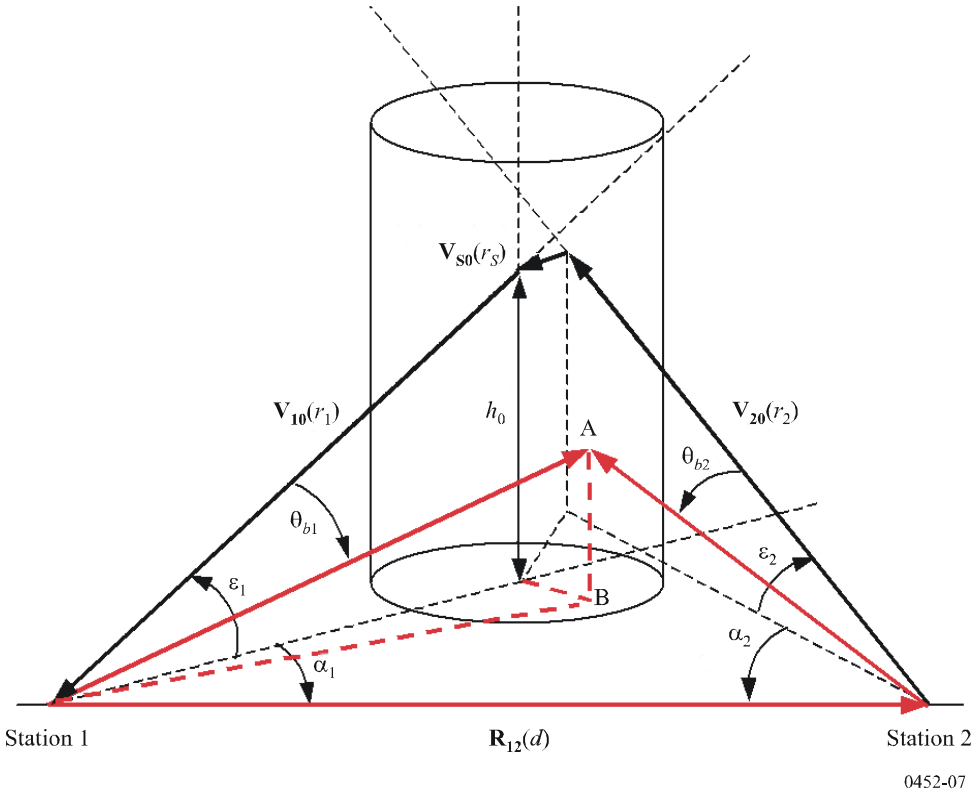

FIGURE 8

Plan view of geometry to determine antenna gains

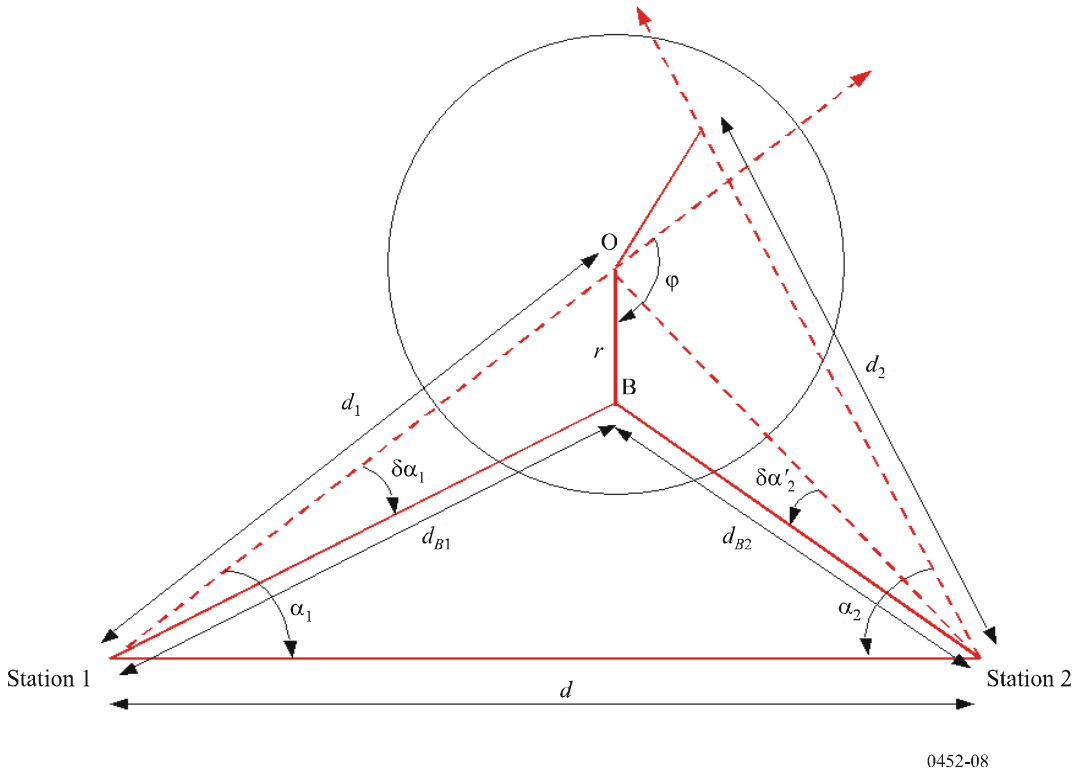

Calculate the horizontal distance from Station 1 to point B:

$$d_{B1} = \sqrt{r^2 + d_1^2 + 2rd_1 \cos\varphi} \qquad \text{km} \tag{77}$$

and the angle between this path and the horizontal projection of the Station 1 antenna main-beam axis:

$$\delta\alpha_1 = \arcsin\left(\frac{r \sin\varphi}{d_{B1}}\right) \tag{78}$$

The elevation angle of point A from Station 1 is given by:

$$\varepsilon_{A1} = \arctan\left(\frac{h}{d_{B1}}\right) \tag{79}$$

The unit-length vector from Station 1 to point A is defined as:

$$\mathbf{V_{A1}} = \begin{bmatrix} \cos\varepsilon_{A1} \cos(\alpha_1 - \delta\alpha_1) \\ -\cos\varepsilon_{A1} \sin(\alpha_1 - \delta\alpha_1) \\ \sin\varepsilon_{A1} \end{bmatrix} \tag{80}$$

Determine the antenna off-axis boresight angle of the point (r, φ, h) for the Station 1 antenna:

$$\theta_{b1} = \arccos\left(\mathbf{V_{A1}} \cdot \mathbf{V_{10}}\right) \tag{81}$$

The distance from Station 1 to point A is:

$$r_{A1} = \frac{d_{B1}}{\cos\varepsilon_{A1}} \quad \text{km} \tag{82}$$

and, noting that the vectors $\mathbf{R_{12}}$, $\mathbf{R_{A2}}$ and $\mathbf{R_{A1}} = r_{A1}\mathbf{V_{A1}}$ form a closed triangle, the vector from Station 2 towards the point A at (r, φ, h) can be found from:

$$\mathbf{R_{A2}} = \mathbf{R_{12}} - r_{A1}\mathbf{V_{A1}} \quad \text{km} \tag{83}$$

The distance from Station 2 to point A is then calculated from:

$$r_{A2} = \left|\mathbf{R_{A2}}\right| \quad \text{km} \tag{84}$$

while the unit vector from Station 1 in the direction of the integration element is:

$$\mathbf{V_{A2}} = \frac{\mathbf{R_{A2}}}{r_{A2}} \tag{85}$$

Then determine the Station 2 antenna off-axis boresight angle of the integration element at point A, with coordinates (r, φ, h):

$$\theta_{b2} = \arccos\left(-\mathbf{V_{A2}} \cdot \mathbf{V_{20}}\right) \tag{86}$$

The above method for determining the antenna gains is appropriate only to circular antennas. Should the Station 1 antenna be a sector or omnidirectional antenna, as deployed in point-to-multipoint broadcast systems, for example, a slightly different method is used to determine the antenna gain, which will vary only in the vertical direction (within the area covered by the rain cell). In this case, the off-axis boresight angle in the vertical direction is determined more simply from:

$$\theta_{b1} = \left|\varepsilon_{A1} - \varepsilon_1\right| \tag{87}$$

Similarly, if the Station 2 antenna is a sector or omnidirectional antenna, the off-axis boresight angle in the vertical direction is determined from:

$$\theta_{b2} = \left|\varepsilon_{A2} - \varepsilon_2\right| \tag{88}$$

where:

$$\varepsilon_{A2} = \arctan\left(\frac{h}{d_{B2}}\right) \tag{89}$$

and:

$$d_{B2} = \sqrt{d^2 + d_{B1}^2 - 2d \cdot d_{B1} \cos(\alpha_1 - \delta\alpha_1)} \quad \text{km} \tag{90}$$

It is important to remember that the off-axis boresight angles are customarily specified in degrees when used in typical antenna radiation patterns, whereas the trigonometrical functions in most software packages generally calculate in radians. A simple conversion from radians to degrees is thus generally necessary before these angles are used in the integration procedures.

The antenna gains can then be obtained from the antenna radiation pattern, from the maximum gain of the antenna and the off-axis boresight angle, which is a function of the location within the rain cell. As a default, the radiation patterns in either Recommendation ITU-R P.620 (also ITU-R F.699) or ITU-R F.1245 can be used, noting that the latter has lower side lobe levels. Note that the gains are required in linear terms for the integration.

Step 5: Determination of path lengths within the rain cell

The path losses from the integration element towards each of the stations, A_1 and A_2, which depend on the path lengths and position of the integration element within the rain cell, are now determined.

The rain cell is divided into three volumes, shown in Fig. 9. In the lower volume, the scattering cross-section is constant throughout the rain cell and is determined by the radar reflectivity Z_R at ground level, with $\zeta(h) = 1$. The paths within the rain cell in the directions toward each station, x_1 and x_2, are subject to attenuation by rain. In the middle volume, the integration element is above the rain height, and the scattering cross-section decreases as a function of height above the rain height, at a rate of −6.5 dB/km. However, a fraction f of each path may still pass through the rain below the rain height, depending on the geometry, and these paths are thus subject to additional attenuation by rain along those fractional path lengths $f_{x1,2}$ which pass through the cell. In the upper volume, the integration element is above the rain cell and no portion of the paths passes through the rain cell below the rain height. Such paths therefore do not suffer any attenuation by rain.

The path lengths in these volumes are now evaluated in the following steps.

Lower volume

In the lower volume, the integration element is always below the rain height h_R, and the paths within the rain cell are all subject to attenuation by rain, i.e.:

$$A_{1,2} = \gamma_{R1,2} x_{1,2} \quad \text{dB} \tag{91}$$

where $\gamma_{R1,2} = k_{1,2} R^{\alpha_{1,2}}$ is the rain specific attenuation, (dB/km), and the coefficients $k_{1,2}$ and $\alpha_{1,2}$ are given as functions of frequency f, polarization τ and path elevation $\varepsilon_{1,2}$ in Recommendation ITU-R P.838. Note that the specific rain attenuation depends on the path elevation angle and, in principle, should be calculated for each integration element for each value of the coordinates (r, φ, h). However, the variation with elevation angle is small, and it is sufficient to determine the values for γ_R only once for the paths toward each station based on the respective antenna elevation angles.

FIGURE 9

Integration volumes within the rain cell

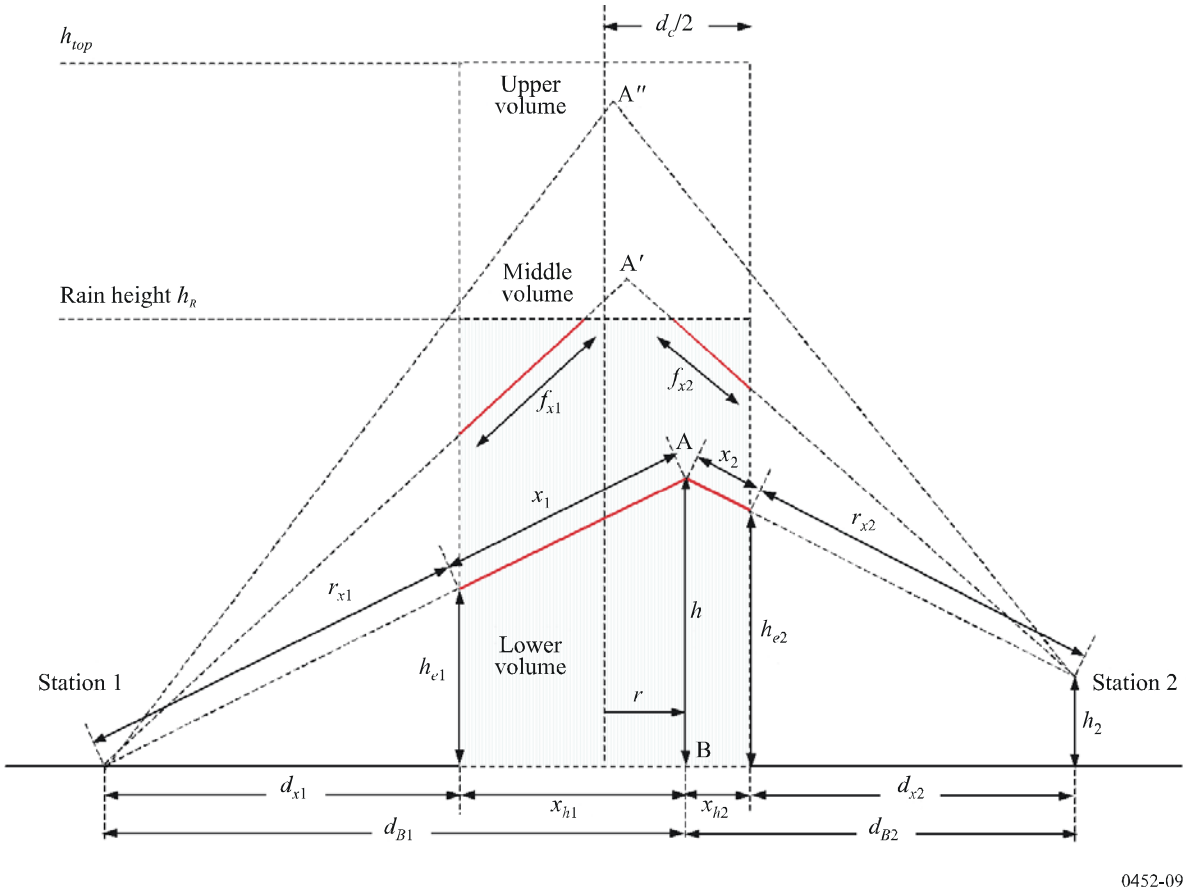

The path lengths r_{x1}, r_{x2}, x_1 and x_2 are derived from the geometry, as follows. Figure 10 shows a horizontal plan view through the ground-plane projection point B of the integration element A. Here, the corrected height of Station 2, h_2, is assumed initially to be zero. This is taken into account later.

Calculate the horizontal distance d_{x1} from Station 1 to the edge of the rain cell (point X_1) is found from the cosine rule (taking the negative sign, since this is to the nearest edge):

$$d_{x1} = d_1 \cos\delta\alpha_1 - \sqrt{d_1^2 \cos^2 \delta\alpha_1 - d_1^2 + \left(\frac{d_c}{2}\right)^2} \quad \text{km} \tag{92}$$

The slant-path distance to the edge of the rain cell is then:

$$r_{x1} = \frac{d_{x1}}{\cos\varepsilon_{A1}} \quad \text{km} \tag{93}$$

FIGURE 10

Plan view of scatter geometry through the integration element

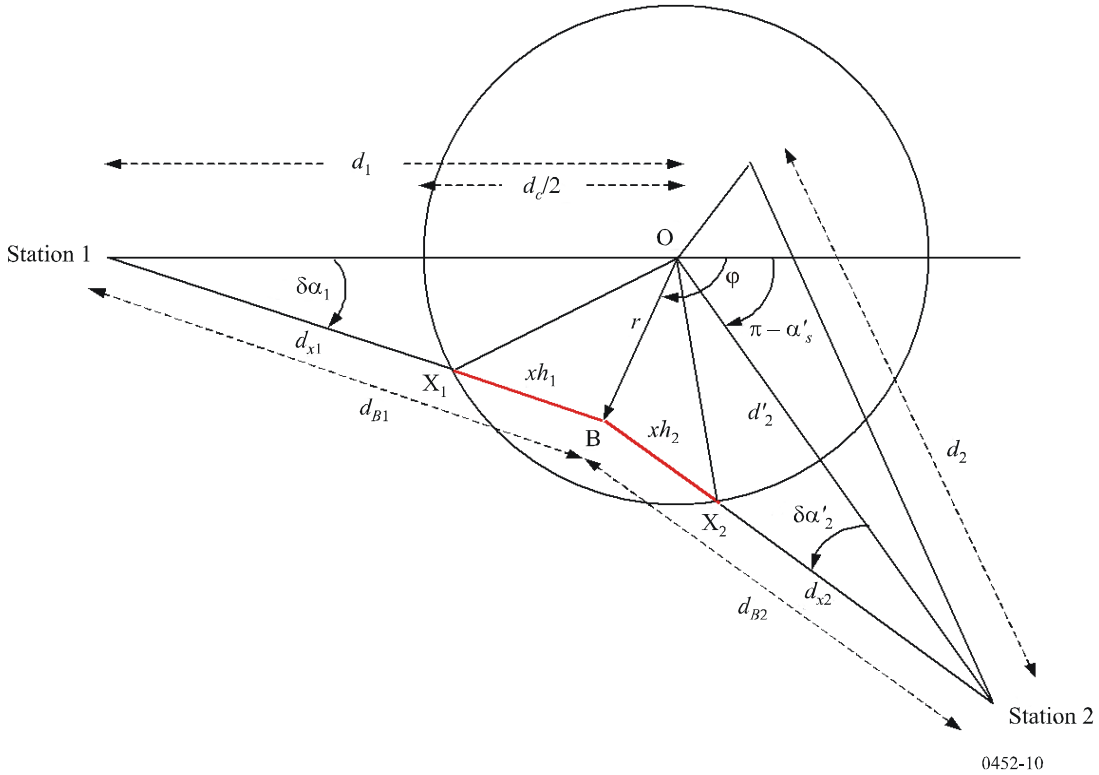

Determine the offset angle of the integration element at point A for Station 2:

$$\delta\alpha_2 = \arctan\left(\frac{-r\sin(\varphi+\alpha'_S)}{d'_2 + r\cos(\varphi+\alpha'_S)}\right) \tag{94}$$

where α'_S is given by:

$$\alpha'_S = \arcsin\left(\frac{d}{d'_2}\sin\alpha_1\right) \tag{95}$$

and

$$d'_2 = \sqrt{d^2 + d_1^2 - 2d\cdot d_1\cos\alpha_1} \quad \text{km} \tag{96}$$

The horizontal distance d_{x2} is then found from the cosine rule:

$$d_{x2} = d'_2\cos\delta\alpha'_2 - \sqrt{\left(\frac{d_c}{2}\right)^2 - d'^2_2\sin^2\delta\alpha'_2} \quad \text{km} \tag{97}$$

Calculate the slant-path distance r_{x2} through the rain cell towards Station 2:

$$r_{x2} = \frac{d_{x2}}{\cos\varepsilon_{A2}} \quad \text{km} \tag{98}$$

Now, two cases need to be considered:

Case 1: when Station 1 is located outside the rain cell, i.e. when $d_1 > d_c/2$. In this case, only a portion of the path from the integration element A to Station 1 will be within the rain cell and hence subject to attenuation;

Case 2: when the elevation angle is very high and Station 1 is located within the rain cell, when $d_1 \le d_c/2$. In this case, the entire path up to the rain height will always be within the rain cell and will thus suffer attenuation.

The path length x_1 for rain attenuation along the path towards Station 1 is determined from the following expression:

$$x_1 = \begin{cases} r_{A1} - r_{x1} & \text{if } d_1 > \dfrac{d_c}{2} \\ r_{A1} & \text{if } d_1 \le \dfrac{d_c}{2} \end{cases} \quad \text{km} \tag{99}$$

and the path length x_2 for rain attenuation along the path towards Station 2 is determined from:

$$x_2 = \begin{cases} r_{A2} - r_{x2} & \text{if } d_2 > \dfrac{d_c}{2} \\ r_{A2} & \text{if } d_2 \le \dfrac{d_c}{2} \end{cases} \quad \text{km} \tag{100}$$

Thus, for cases where the integration element is below the rain height, the attenuation through the rain cell can be determined, in linear terms, from:

$$A_b = \exp\left[-k\left(\gamma_{R1} x_1 + \gamma_{R2} x_2\right)\right] \qquad \text{if } h \le h_R \tag{101}$$

where $k = 0.23026$ is a constant to convert attenuation in dB to Nepers.

Middle and upper volumes

In these volumes, the integration element is above the rain height, h_R, but some portions of the paths towards each of the stations may pass through the rain below h_R. This will occur only when the elevation angles of the integration element A, $\varepsilon_{A1,2}$, is less than the angles $\varepsilon_{C1,2}$ subtended at each station by the nearest upper corner of the rain cell, i.e. if:

$$\varepsilon_{A1} < \varepsilon_{C1} = \arctan\left(\frac{h_R}{d_{x1}}\right) \quad \text{and} \quad \varepsilon_{A2} < \varepsilon_{C2} = \arctan\left(\frac{h_R - h_2}{d_{x2}}\right)$$

In these cases, the resultant attenuation must be taken into account. This is particularly relevant for Case 2 above, when one of the antennas has a very high elevation angle and the station is located within the rain cell.

From Fig. 9, the heights at which the rays from the integration element at point A pass through the edges of the rain cell can be determined from the ratios of the horizontal distances from each station to the edge of the rain cell and to point B:

$$\begin{aligned} h_{e1} &= h \cdot \frac{d_{x1}}{d_{B1}} \\ h_{e2} &= \left(h - h_2\right) \cdot \frac{d_{x2}}{d_{B2}} + h_2 \end{aligned} \quad \text{km} \tag{102}$$

The fractional of the path lengths $fx_{1,2}$ which pass through the rain cell can then be determined from ratios:

$$f_{x1,2} = \begin{cases} x_{1,2}\left(\dfrac{h_R - h_{e1,2}}{h - h_{e1,2}}\right) & \text{if } h > h_R > h_{e1,2} \quad \text{and } \varepsilon_{A1,2} < \varepsilon_{C1,2} \\ 0 & \text{otherwise} \end{cases} \quad \text{km} \qquad (103)$$

Finally, calculate the attenuation, in linear terms, for cases where the integration element is above the rain height, h_R:

$$A = \exp\left[-k\left\{6.5(h - h_R) + \gamma_{R1} f_{x1} + \gamma_{R2} f_{x2}\right\}\right] \qquad \text{for } h \geq h_R \qquad (104)$$

This Step then defines the integrand for the scatter transfer function.

Step 6: Attenuation outside the rain cell

In the formulation used here, rain is confined solely to a cell with diameter d_c, defined by the geometry in Step 2, and the rainfall rate is considered uniform within that cell. In general, the rain will extend beyond this region, decreasing in intensity as the distance from the cell centre increases, and this must be taken into account. However, if the station is located inside the rain cell, then there will be no external rain attenuation to be considered for that station. Furthermore, if the integration element is sufficiently far above the rain height that no part of the path to either station passes through the rain cell, then no external attenuation is included along that path.

As an approximation, the rain outside the rain cell is assumed to decay with a scaling distance defined by:

$$r_m = 600 R^{-0.5} 10^{-(R+1)^{0.19}} \qquad \text{km} \qquad (105)$$

For scattering below the rain height, calculate the attenuation outside the rain cell using the following expression:

$$A_{ext1,2} = \begin{cases} \dfrac{\gamma_{R1,2} r_m}{\cos \varepsilon_{A1,2}} \left[1 - \exp\left(\dfrac{d_{x1,2}}{r_m}\right)\right] & \text{if } d_{1,2} > \dfrac{d_c}{2} \quad \text{and} \quad f_{x1,2} \neq 0 \\ 0 & \text{if } d_{1,2} \leq \dfrac{d_c}{2} \quad \text{or} \quad f_{x1,2} = 0 \end{cases} \quad \text{dB} \qquad (106)$$

i.e., the attenuation along either path is set to zero if the relevant station is located within the rain cell ($d_1 \leq d_c/2$) or if the integration element is above the rain cell and no part of the path passes through the rain cell, determined by whether or not the fractional paths $f_{x1,2}$ are zero.

Step 7: Numerical integration of the scatter transfer function

The integration is split into two sections, for scattering below the rain height and for scattering above the rain height:

$$C_b = \int_{h_{\min}}^{h_R} \int_0^{2\pi} \int_0^{\frac{d_c}{2}} \frac{G_1 G_2}{r_{A1}^2 r_{A2}^2} \exp\left[-k\left(\gamma_{R1} x_1 + \gamma_{R2} x_2 + A_{ext1} + A_{ext2}\right)\right] \cdot r \, dr \, d\varphi \, dh \qquad (107)$$

$$C_a = \int_{h_R}^{h_{top}} \int_0^{2\pi} \int_0^{\frac{d_c}{2}} \frac{G_1 G_2}{r_{A1}^2 r_{A2}^2} \exp\left[-k\left(6.5(h - h_R) + \gamma_{R1} f_{x1} + \gamma_{R2} f_{x2} + A_{ext1} + A_{ext2}\right)\right] \cdot r \, dr \, d\varphi \, dh \qquad (108)$$

where the antenna gains are specified in linear terms, as functions of the off-axis boresight angles $\theta_{b1,2}(r, \varphi, h)$.

The integration, in cylindrical coordinates, is carried out over the ranges: for r from 0 to the radius of the rain cell, $d_c/2$, and for φ from 0 to 2π. Some constraints can be placed on the third integration variable, h, the height within the rain cell. The minimum height, h_{min}, is determined by the visibility of the rain cell from each of the stations. If there be any shielding from terrain in the vicinity of either station, then scattering from heights within the rain cell which are not visible from either station should be precluded from the integration. The minimum height for integration can thus be determined from the horizon angles for each station, as:

$$h_{min} = \max\left(d_{x1} \tan \varepsilon_{H1}, d_{x2} \tan \varepsilon_{H2}\right) \quad \text{km} \tag{109}$$

Note that local values are used here, since any inherent shielding due to the Earth's curvature at zero elevation is already taken into account in determining the off-axis boresight angles.

The maximum height for integration, h_{top}, can be defined, in order to minimize the computational requirements, since it will not, in general, be necessary to integrate the scattering cross-section at heights above which the antenna side lobe levels are significantly reduced. As a default value, the height above which the integration may be terminated without loss of accuracy is assumed to be 15 km.

Numerical integration: There are many methods available for numerical integration, and numerous mathematical software packages include intrinsic integration functions which can be exploited effectively. Where the user wishes to develop a dedicated package in other programming languages, methods based on iterative bisection techniques have proved effective. One such technique is the Romberg method, which is a higher-order variant of the basic trapezoidal (i.e. Simpson's) rule for integration by successive bisections of the integration intervals.

Romberg integration uses a combination of two numerical methods to calculate an approximation to a proper integral, i.e.:

$$I = \int_a^b y(x)\mathrm{d}x$$

The extended trapezoidal rule is used to calculate a sequence of approximations to the integral with the intervals between function evaluations being divided by two between each term. Polynomial extrapolation is then used to extrapolate the sequence to a zero-length interval. The method can be summarized by the pseudo-code loop:

Index = 1
WHILE estimated_error > desired_error DO
    S(*Index*) = Trapezoidal Rule Approximation using 2^{Index} intervals
    I = Polynomial Extrapolation of S
    Index = *Index* + 1
ENDWHILE

The extended trapezoidal rule

By linearly interpolating between $N + 1$ equally spaced abscissae (x_i, y_i) the integral can be approximated:

$$I \approx T^N = h(N)\left(\frac{1}{2}y_0 + y_1 \cdots y_{N-1} + \frac{1}{2}y_N\right)$$

where:

$h(N)=\frac{b-a}{N}$: interval between abscissae.

The number of intervals can be doubled using the recursion:

$$T^{2N}=\frac{1}{2}T^{N}+h(2N)(y_1+y_3\cdots y_{N-3}+y_{N-1})$$

The Romberg method recursively builds a sequence: $S(i)=T^{2^i}$.

Polynomial extrapolation: In the limit, the error in the extended trapezoidal approximation to I is a polynomial in h^2, i.e.:

$$I=T^{N}+\varepsilon^{N}$$

where:

$$\varepsilon^{N}\cong P(h^2(N))$$

and

P: is an unknown polynomial.

The sequence of trapezoidal approximations, $T^N=\varepsilon^N$, is also a polynomial in h^2 and so polynomial extrapolation may be used to estimate the limit as $h\to 0$. If m trapezoidal approximations are available, then a unique polynomial of degree $M-1$ may be fitted to the points $(h^2(n),T^n)$ for $n=1,2,4,8,\cdots,2^{M-1}$. Evaluating this unique polynomial at $h=0$ yields an approximation to the limit of the trapezoidal method.

Usually Neville's method is used to calculate the value of the polynomial at $h = 0$. Neville's method is efficient and yields an error estimate which may be used to terminate the Romberg integration. The method is a successive linear interpolation approximation to high degree Lagrangian polynomial interpolation. The Lagrange method can be described as follows. For $M + 1$ points (x_i,y_i), a polynomial of degree m can be defined as a linear combination of basic functions:

$$P(x)\equiv\sum_{i=0}^{n}y_iL_i(x_i)\equiv\sum_{i=0}^{n}y_i\prod_{\substack{k=0\\k\neq i}}^{n}\frac{(x-x_k)}{(x_i-x_k)}$$

i.e.

$$L_i(x)=\frac{(x-x_0)\ldots(x-x_{i-1})(x-x_{i+1})\ldots(x-x_n)}{(x_i-x_0)\ldots(x_i-x_{i-1})(x_i-x_{i+1})\ldots(x_i-x_n)}$$

This interpolation method requires all ordinates y_i to be known in order to find an estimate of the solution at $x = 0$, and for large problems this is not efficient, since it does not exploit previous interpolations when iterating to higher orders. Neville's method is a recursive process based on the relationship between one approximation to a polynomial and its two preceding approximations. Thus, for any two points(x_k,y_k), there is a unique polynomial of degree 0, i.e. a straight line, passing through those two points, $P_k=y_k$. A second iteration is performed in which the polynomial is fitted

through pairs of point yielding $P_{12}, P_{23}, \ldots$, and the procedure repeated to build up a pyramid of approximations:

$$\begin{array}{ccccc} P_1 & & & & \\ & P_{12} & & & \\ P_2 & & P_{123} & & \\ & P_{23} & & P_{1234} & \\ P_3 & & P_{234} & & \\ & P_{34} & & & \\ P_4 & & & & \end{array}$$

The final result can then be represented as:

$$P_{i(i+1)\ldots(i+m)} = \frac{(x - x_{i+m})P_{i(i+1)\ldots(i+m-1)} + (x_i - x)P_{(i+1)(i+2)\ldots(i+m)}}{x_i - x_{i+m}}$$

Neville's method is thus a recursive process to complete the pyramid column-by-column, in a computationally efficient way.

In practice, the polynomial extrapolation becomes unstable when large numbers of points are fitted and so typically in Romberg integration, fourth degree polynomial extrapolation is used, fitting to the last five trapezoidal approximations.

Numerical integration methods, such as those which use bisection techniques, iterate until an accuracy (precision) criterion is met, whereby the iteration is terminated when the difference between successive iterations is smaller than a predetermined fraction of the previous result. Typically, this fraction will be between 10^{-3} and 10^{-6}, the latter value being close to the capabilities of 32-bit processors. Care should be taken when using larger values above this range, since errors in the calculated losses may increase. As a general guide, a value of 10^{-4} is found to be a good compromise between accuracy and computational speed.

Three nested numerical integrations are required in order to carry out the three-dimensional volume integration over the rain cell, in cylindrical coordinates, with the outer integration being over the height parameter h, for example. This integration calls for the integral over the azimuthal parameter φ at a particular value of h, which in turn calls for the integral over the radius parameter, r, for particular values of (h, φ).

It should be noted that many iterations of the scatter transfer function are generally necessary in order to achieve the required precision, especially in cases where antenna gains are high and the product of the antenna gains can vary across the diameter of the rain cell by 60 dB or more. Computation times can therefore be many tens of minutes and even hours for more extreme cases, even with high-speed processors.

A software version of the methodology written in Fortran, which employs the Romberg method, and a version written in Mathcad, using inbuilt integration facilities, is available from the Radiocommunication Bureau.

Step 8: Determination of other loss factors

Calculate the deviation from Rayleigh scattering using equation (39) with the scattering angle φ_S given by equation (54).

Calculate the attenuation along the paths due to absorption by atmospheric gases using Annex 2 of Recommendation ITU-T R P.676 for the specific attenuations γ_o and γ_w and the equivalent heights h_o and h_w for dry air and water vapour respectively. The attenuations are determined using the following expressions for path attenuation between two altitudes above sea level, with the upper altitude being determined by the height of the quasi-intersection point between the two antenna

beam main axes. This method is an approximation, since the actual gaseous attenuation will vary for each scattering element within the scattering volume. However, since gaseous attenuation is generally a minor component in the overall transmission loss, and its variability is small, when compared with the uncertainties in other parameters such as rainfall rates, rain heights, and the geometry of the rain cell itself, this simplification is considered justifiable. The following method provides estimates of the gaseous attenuation with acceptable accuracy for the overall procedure.

The lower altitudes for each station are given by the local values $h_{1\_loc} = h_{2\_loc}$. The upper altitude h_p is the height of the quasi-intersection point, taking into account the Earth's curvature, i.e. the local value, which is found from:

$$h_p = h_0 + \sqrt{d_1^2 + r_{eff}^2} - r_{eff} + h_c \qquad \text{km} \tag{110}$$

For elevation angles between 5° and 90°, the attenuation between two altitudes is determined from the difference between the total slant-path attenuations from each altitude:

$$A_{o\_i} = \frac{\gamma_o h_o - \gamma_o h_o \left[\exp\left(-\frac{h_{i\_loc}}{h_o} \right) - \exp\left(-\frac{h_p}{h_0} \right) \right]}{\sin \varepsilon_{i\_loc}} \qquad \text{dB} \tag{111}$$

$$A_{w\_i} = \frac{\gamma_w h_o - \gamma_w h_o \left[\exp\left(-\frac{h_{i\_loc}}{h_w} \right) - \exp\left(-\frac{h_p}{h_w} \right) \right]}{\sin \varepsilon_{i\_loc}} \qquad \text{dB} \tag{112}$$

where the index, i, refers to each of the two stations and ε_{i_loc} are the local elevation angles of each antenna.

The water-vapour density, ρ, used to determine the specific attenuation γ_w is the hypothetical sea-level value found from the ground-level value at the stations (which can be assumed to be the same):

$$\rho = \rho_g \exp\left(\frac{h_{i\_loc}}{2} \right) \qquad \text{g/m}^3 \tag{113}$$

For elevation angles between 0° and 5°, it is necessary to take into account the effects of refraction. The elevation angles for the upper path are determined from:

$$\varepsilon'_i = \arccos\left(\frac{h_1 + r_{eff}}{h_p + r_{eff}} \cos \varepsilon_{i\_loc} \right) \tag{114}$$

The path attenuation is then given by the following expressions:

For dry air attenuation:

$$A_{o\_i} = \gamma_o \sqrt{h_o} \left[\frac{\sqrt{h_{i\_loc} + r_{eff}} \cdot F\left(\tan\varepsilon_i \sqrt{\frac{h_{i\_loc} + r_{eff}}{h_o}} \right) \exp\left(-\frac{h_{i\_loc}}{h_o} \right)}{\cos\varepsilon_{i\_loc}} - \frac{\sqrt{h_p + r_{eff}} \cdot F\left(\tan\varepsilon'_i \sqrt{\frac{h_p + r_{eff}}{h_o}} \right) \exp\left(-\frac{h_p}{h_o} \right)}{\cos\varepsilon'_i} \right] \quad \text{dB} \qquad (115)$$

and for water-vapour attenuation:

$$A_{w\_i} = \gamma_w \sqrt{h_w} \left[\frac{\sqrt{h_{i\_loc} + r_{eff}} \cdot F\left(\tan\varepsilon_i \sqrt{\frac{h_{i\_loc} + r_{eff}}{h_w}} \right) \exp\left(-\frac{h_{i\_loc}}{h_w} \right)}{\cos\varepsilon_{i\_loc}} - \frac{\sqrt{h_p + r_{eff}} \cdot F\left(\tan\varepsilon'_i \sqrt{\frac{h_p + r_{eff}}{h_w}} \right) \exp\left(-\frac{h_p}{h_w} \right)}{\cos\varepsilon'_i} \right] \quad \text{dB} \qquad (116)$$

where the function, F, is defined by:

$$F(x) = \frac{1}{0.661x + 0.339\sqrt{x^2 + 5.51}} \qquad (117)$$

Include also any polarization mismatch, M, which is appropriate.

Step 9: Determination of the cumulative distribution of transmission loss

For each pair of rainfall rate and rain height values, calculate the transmission loss according to Steps 5 to 8, using the following expression:

$$L = 208 - 20\log f - 10\log Z_R - 10\log(C_b + C_a) + 10\log S + A_g - M \quad \text{dB} \qquad (118)$$

After all possible combinations of rainfall rate and rain height have been evaluated, the resulting values of transmission loss (dB) are then truncated to the nearest higher integer dB value (using, for example a *ceiling* function), and the probabilities (in percentage terms) of all those combinations which yield the same loss are summed together, to derive the overall probability for each level of transmission loss. The resulting probability density function is then converted to the corresponding cumulative distribution of transmission loss, by summing the percentages for increasing values of loss.

Appendix 1
to Annex 1

Radio-meteorological data required for the clear-air prediction procedure

1 Introduction

The clear-air prediction procedures rely on radio-meteorological data to provide the basic location variability for the predictions. These data are provided in the form of maps which are contained in this Appendix.

2 Maps of vertical variation of radio refractivity data

For the global procedure, the clear-air radio-meteorology of the path is characterized for the continuous (long-term) interference mechanisms by the average annual value of ΔN (the refractive index lapse-rate over the first 1 km of the atmosphere) and for the anomalous (short-term) mechanisms by the time percentage, β_0%, for which the refractive gradient of the lower atmosphere is below −100 N-units/km. These parameters provide a reasonable basis upon which to model the clear-air propagation mechanisms described in § 2 of Annex 1. For some of these quantities, data are provided in this Appendix for annual and worst-month calculations:

– Figure 11 provides average year ΔN data;

– Figure 12 provides the associated maximum monthly mean ΔN contours.

FIGURE 11

Average annual values of ΔN

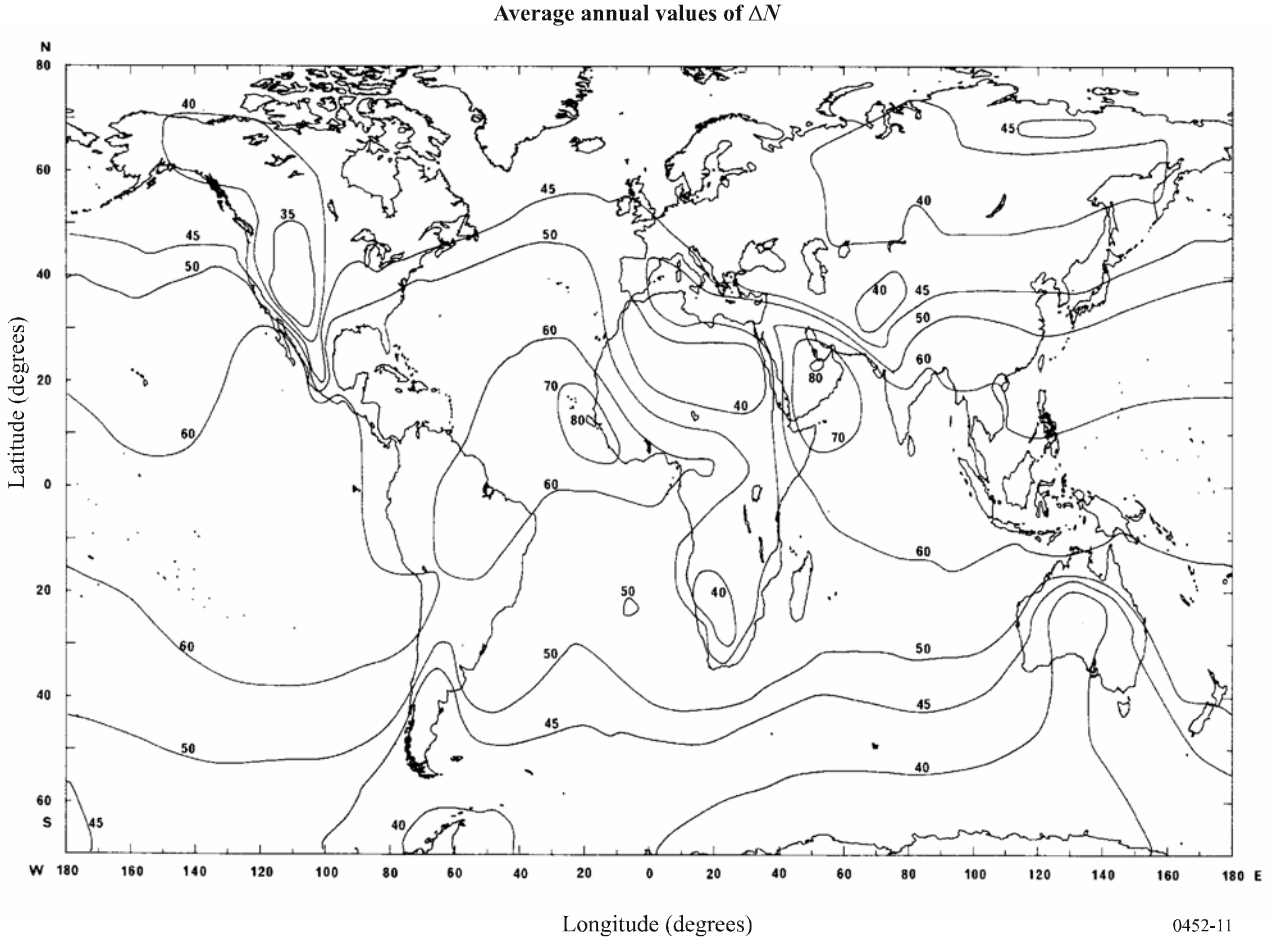

FIGURE 12

Maximum monthly mean values of ΔN (for worst-month prediction)

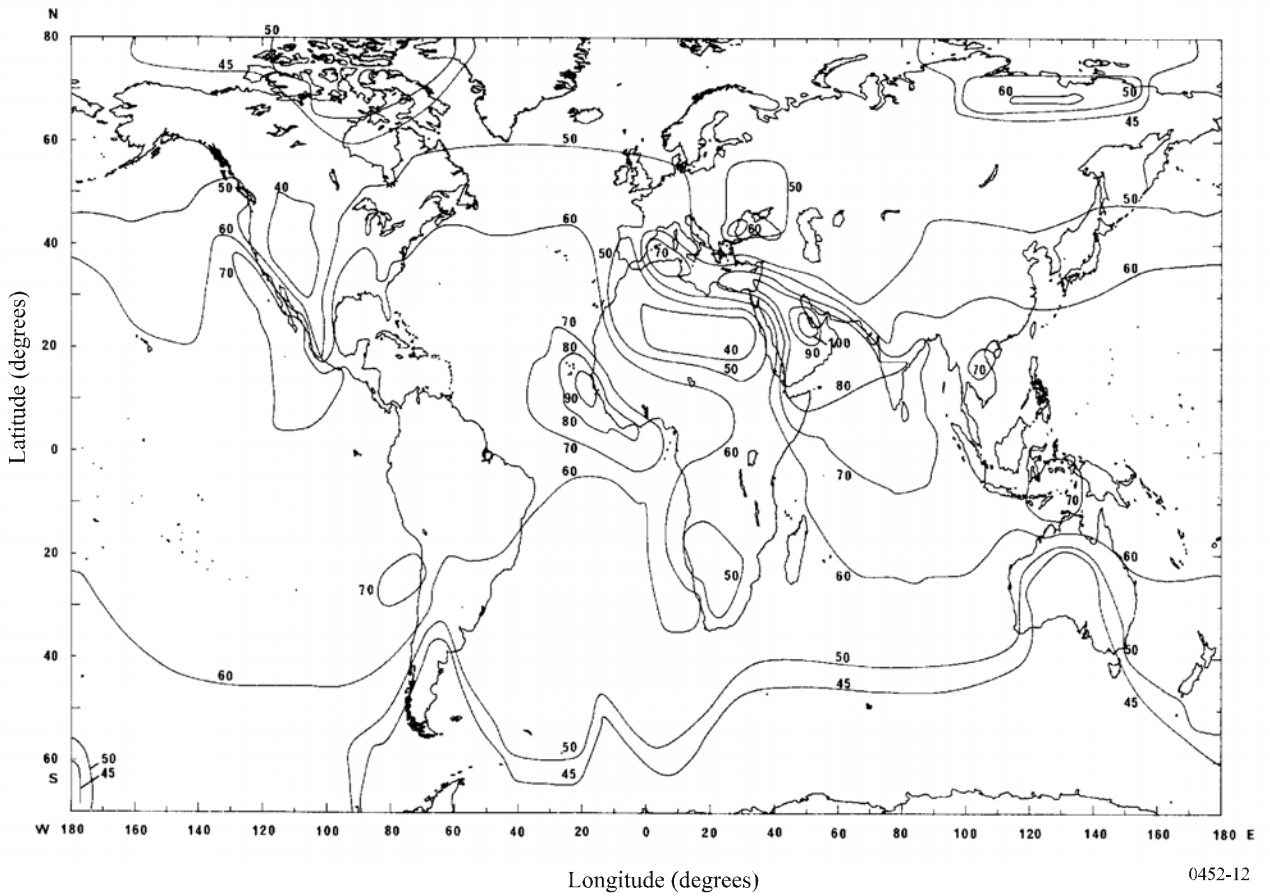

3 Map of surface refractivity, N_0

Figure 13 provides a map of average sea-level surface refractivity, N_0, for the troposcatter model.

4 Implementation of maps in computer database form

For computer implementation of the procedures, it is convenient to capture these maps in digital form and to convert them into simple databases that can be accessed by the software.

For the global refractive index maps, it is suggested that the contours be converted into two-dimensional arrays of 0.5×0.5 latitude and longitude. To avoid discontinuities in the prediction with small changes in location or distance the values for each array cell should be derived by interpolation between the contours.

FIGURE 13

Sea-level surface refractivity, N_0

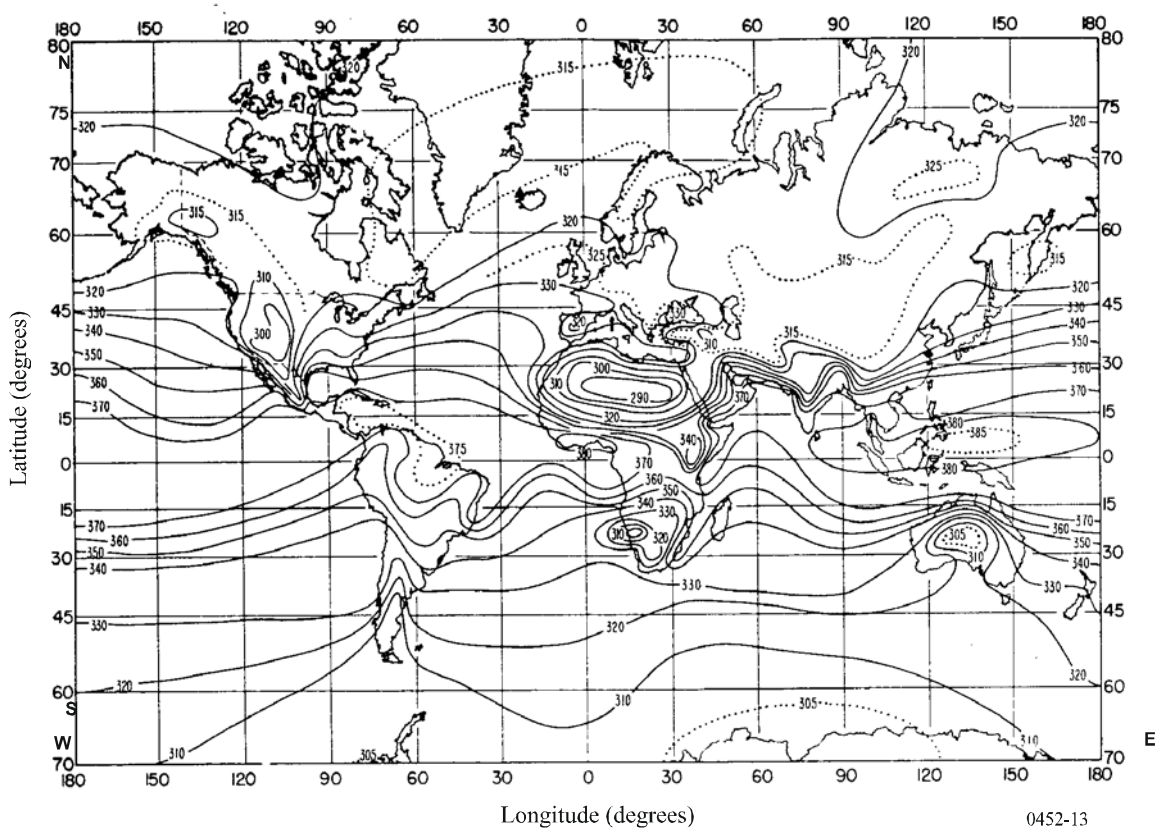

Appendix 2
to Annex 1

Path profile analysis

1 Introduction

For path profile analysis, a path profile of terrain heights above mean sea level is required. The parameters that need to be derived from the path profile analysis for the purposes of the propagation models are given in Table 9.

2 Construction of path profile

Based on the geographical coordinates of the interfering (φ_t, ψ_t) and interfered-with (φ_r, ψ_r) stations, terrain heights (above mean sea level) along the great-circle path should be derived from a topographical database or from appropriate large-scale contour maps. The preferred distance resolution of the profile is that giving an integer number of steps of approximately 0.25 km. Other distance increments can be used, up to a maximum of about 1 km, with some possible decrease in prediction accuracy. The profile should include the ground heights at the interfering and

interfered-with station locations as the start and end points. To the heights along the path should be added the necessary Earth's curvature, based on the value of a_e found in equation (6).

Although equally-spaced profile points are considered preferable, it is possible to use the method with non-equally-spaced profile points. This may be useful when the profile is obtained from a digital map of terrain height contours. However, it should be noted that the Recommendation has been developed from testing using equally-spaced profile points; information is not available on the effect of non-equally-spaced points on accuracy.

For the purposes of this Recommendation the point of the path profile at the interferer is considered as point zero, and the point at the interfered-with station is considered as point n. The path profile therefore consists of $n + 1$ points. Figure 14 gives an example of a path profile of terrain heights above mean sea level, showing the various parameters related to the actual terrain.

FIGURE 14

Example of a (trans-horizon) path profile

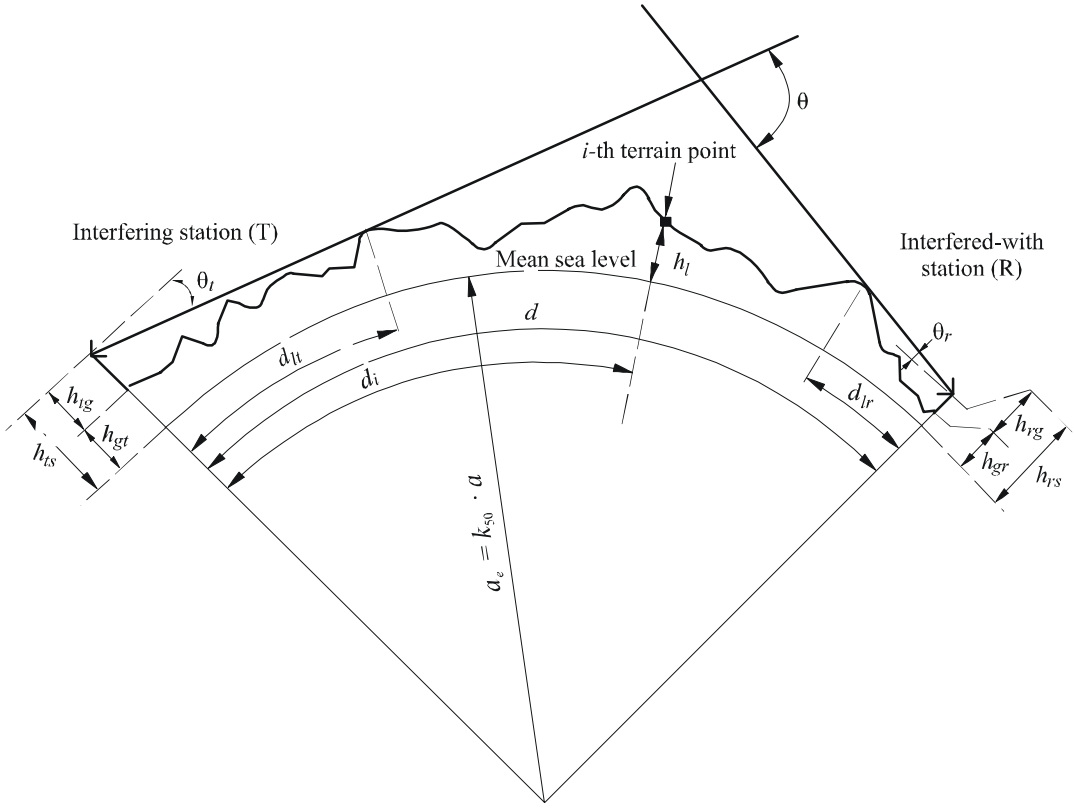

Note 1 – The value of θ_t as drawn will be negative.

0452-14

Table 9 defines parameters used or derived during the path profile analysis.

TABLE 9

Path profile parameter definitions

Parameter	Description
a_e	Effective Earth's radius (km)
d	Great-circle path distance (km)
d_i	Great-circle distance of the i-th terrain point from the interferer (km)
d_{ii}	Incremental distance for regular path profile data (km)
f	Frequency (GHz)
λ	Wavelength (m)
h_{ts}	Interferer antenna height (m) above mean sea level (amsl)
h_{rs}	Interfered-with antenna height (m) (amsl)
θ_t	Horizon elevation angle above local horizontal (mrad), measured from the interfering antenna
θ_r	Horizon elevation angle above local horizontal (mrad), measured from the interfered-with antenna
θ	Path angular distance (mrad)
h_{st}	Height of the smooth-Earth surface (amsl) at the interfering station location (m)
h_{sr}	Height of the smooth-Earth surface (amsl) at the interfered-with station location (m)
h_i	Height of the i-th terrain point amsl (m) h_0: ground height of interfering station h_n: ground height of interfered-with station
h_m	Terrain roughness (m)
h_{te}	Effective height of interfering antenna (m)
h_{re}	Effective height of interfered-with antenna (m)

3 Path length

For general cases the path length, d (km), can be found from the path profile data:

$$d = \sum_{i=1}^{n} (d_i - d_{i-1}) \quad \text{km} \tag{119}$$

however, for regularly-spaced path profile data this simplifies to:

$$d = n \cdot d_{ii} \quad \text{km} \tag{120}$$

where d_{ii} is the incremental path distance (km).

4 Path classification

The path profile must next be used to classify the path into one of three geometrical categories based on an effective Earth's radius of a_e. The interference path classifications are as indicated in Table 4.

4.1 Classification Step 1: Test for a trans-horizon path

A path is trans-horizon if the physical horizon elevation angle as seen by the interfering antenna (relative to the local horizontal) is greater than the angle (again relative to the interferer's local horizontal) subtended by the interfered-with antenna.

The test for the trans-horizon path condition is thus:

$$\theta_{max} > \theta_{td} \quad \text{mrad} \tag{121}$$

where:

$$\theta_{max} = \max_{i=1}^{n-1} (\theta_i) \quad \text{mrad} \tag{122}$$

θ_i: elevation angle to the i-th terrain point

$$\theta_i = \frac{h_i - h_{ts}}{d_i} - \frac{10^3 \, d_i}{2 \, a_e} \quad \text{mrad} \tag{123}$$

where:

h_i: height of the i-th terrain point (m) amsl

h_{ts}: interferer antenna height (m) amsl

d_i: distance from interferer to the i-th terrain element (km)

$$\theta_{td} = \frac{h_{rs} - h_{ts}}{d} - \frac{10^3 \, d}{2 \, a_e} \quad \text{mrad} \tag{124}$$

where:

h_{rs}: interfered-with antenna height (m) amsl

d: total great-circle path distance (km)

a_e: median effective Earth's radius appropriate to the path (equation (6)).

If the condition of equation (121) is met, then the remaining path profile analysis required for trans-horizon paths can be undertaken (see § 5.1). Under these conditions Step 2 of the path classification is not needed.

If the condition of equation (121) is not fulfilled, the path is line-of-sight, with or without incursion by the terrain of the first Fresnel zone.

4.2 Step 2: Test for line-of-sight with sub-path diffraction (i.e. without full first Fresnel zone clearance)

A non trans-horizon path is line-of-sight with sub-path diffraction, if the elevation angle over the physical horizon, as seen by the interfering antenna (relative to the local horizontal), and allowing for clearance equal to the first Fresnel ellipsoid radius at the horizon point, is greater than the angle (again relative to the interferer's local horizontal) subtended by the interfered-with antenna.

The path has sub-path diffraction if:

$$\theta_{fmax} > \theta_{td} \quad \text{mrad} \tag{125}$$

where:

$$\theta_{fmax} = \max_{i=1}^{n-1} (\theta_{fi}) \tag{126}$$

To complete this test an extra term is therefore required in equation (123) to allow for the first Fresnel ellipsoid. Recommendation ITU-R P.526, § 2, gives the radius of this ellipsoid, R_i (m), at any point along the path:

$$R_i = 17.392 \sqrt{\frac{d_i (d - d_i)}{d \cdot f}} \quad \text{m} \tag{127}$$

where f is the frequency (GHz).

The appropriate radius, R_i (m), is added to each terrain height, h_i (m), in equation (123) yielding equation (128). Allowing for first Fresnel zone clearance, θ_{fi}, the terminal antenna elevation angle (rad) to the i-th point is obtained from the following equation:

$$\theta_{fi} = \frac{(h_i + R_i) - h_{ts}}{d_i} - \frac{10^3 \, d_i}{2 \, a_e} \quad \text{mrad} \tag{128}$$

If the condition of equation (125) is met, then the remaining path profile analysis required for sub-path diffraction cases can be undertaken.

If the condition of equation (125) is not fulfilled, the path is line-of-sight and no further path profile analysis is needed.

5 Derivation of parameters from the path profile

5.1 Trans-horizon paths

The parameters to be derived from the path profile are those contained in Table 9.

5.1.1 Interfering antenna horizon elevation angle, θ_t

The interfering antenna's horizon elevation angle is the maximum antenna horizon elevation angle when equation (122) is applied to the $n - 1$ terrain profile heights.

$$\theta_t = \theta_{max} \quad \text{mrad} \tag{129}$$

with θ_{max} as determined in equation (122).

5.1.2 Interfering antenna horizon distance, d_{lt}

The horizon distance is the minimum distance from the transmitter at which the maximum antenna horizon elevation angle is calculated from equation (122).

$$d_{lt} = d_i \quad \text{km} \quad \text{for max } (\theta_i) \tag{130}$$

5.1.3 Interfered-with antenna horizon elevation angle, θ_r

The receive antenna horizon elevation angle is the maximum antenna horizon elevation angle when equation (122) is applied to the $n - 1$ terrain profile heights.

$$\theta_r = \max_{j=1}^{n-1} (\theta_j) \quad \text{mrad} \tag{131}$$

$$\theta_j = \frac{h_j - h_{rs}}{d - d_j} - \frac{10^3 \, (d - d_j)}{2 \, a_e} \quad \text{mrad} \tag{132}$$

5.1.4 Interfered-with antenna horizon distance, d_{lr}

The horizon distance is the minimum distance from the receiver at which the maximum antenna horizon elevation angle is calculated from equation (122).

$$d_{lr} = d - d_j \quad \text{km} \quad \text{for max } (\theta_j) \tag{133}$$

5.1.5 Angular distance θ (mrad)

$$\theta = \frac{10^3\ d}{a_e} + \theta_t + \theta_r \quad \text{mrad} \tag{134}$$

5.1.6 "Smooth-Earth" model and effective antenna heights

5.1.6.1 General

To determine the effective antenna heights, and to allow an appropriate assessment of the path roughness to be made, it is necessary to derive an effective "smooth-Earth" surface as a reference plane over which the irregular terrain of the path is deemed to exist. Once this is derived the values of the terrain roughness parameter (§ 5.1.6.4) and effective antenna heights for the interfering and interfered-with stations can be obtained.

5.1.6.2 Exceptions

For straightforward "sea" paths, i.e. $\omega \geq 0.9$, and where both antenna horizons fall on the sea surface, the derivation of the smooth-Earth surface calculation can be omitted if required. In such case the reference plane can be taken to be a mean sea (or water) level over the whole path, the terrain roughness may be assumed to be 0 m, and the effective antenna heights are equal to the real heights above the sea surface.

For all other paths it is necessary to apply the smooth-Earth terrain approximation procedure detailed in § 5.1 and to derive the effective antenna heights and the terrain roughness as in § 5.1.6.4.

5.1.6.3 Deriving the smooth-Earth surface

Derive a straight line approximation to the terrain heights amsl of the form:

$$h_{si} = h_{st} + m \cdot d_i \quad \text{m} \tag{135}$$

where:

h_{si}: height (m) amsl, of the least-squares fit surface at distance d_i (km) from the interference source

h_{st}: height (m) amsl, of the smooth-Earth surface at the path origin, i.e. at the interfering station

m: slope (m/km) of the least-squares surface relative to sea level.

Alternative methods are available for the next two steps in the calculation. Equations (136a) and (137a) may be used if the profile points are equally spaced. Equations (136b) and (137b), which are more complicated, must be used if the profile points are not equally spaced, and may be used in either case.

For equally spaced profiles:

$$m = \frac{\sum_{i=0}^{n} (h_i - h_a)\left(d_i - \frac{d}{2}\right)}{\sum_{i=0}^{n}\left(d_i - \frac{d}{2}\right)^2} \quad \text{m/km} \tag{136a}$$

For any profile:

$$m = \left(\frac{1}{d^3}\right)\sum_{i=1}^{n} 3\,(d_i - d_{i-1})\,(d_i + d_{i-1} - d)\,(h_i + h_{i-1} - 2h_a) + (d_i - d_{i-1})^2\,(h_i - h_{i-1}) \quad \text{m/km} \tag{136b}$$

where:

h_i: real height of the i-th terrain point (m) amsl

h_a: mean of the real path heights amsl from h_0 to h_n inclusive (m) given by:

For equally-spaced profiles:

$$h_a = \frac{1}{n+1}\sum_{i=0}^{n} h_i \quad \text{m} \tag{137a}$$

For any profile a weighted mean is calculated:

$$h_a = \left(\frac{1}{2d}\right)\sum_{i=1}^{n}(d_i - d_{i-1})\,(h_i + h_{i-1}) \quad \text{m} \tag{137b}$$

The height of the smooth-Earth surface at the interfering station, h_{st}, is then given by:

$$h_{st} = h_a - m\frac{d}{2} \quad \text{m} \tag{138}$$

and hence the height of the smooth-Earth surface at the interfered-with station, h_{sr}, is given by:

$$h_{sr} = h_{st} + m \cdot d \quad \text{m} \tag{139}$$

Correction must then be made if the smooth-Earth heights fall above the true ground height, i.e.:

$$h_{st} = \min\,(h_{st}, h_0) \quad \text{m} \tag{140a}$$

$$h_{sr} = \min\,(h_{sr}, h_n) \quad \text{m} \tag{140b}$$

If either or both of h_{st} or h_{sr} were modified by equations (140a) or (140b) then the slope, m, of the smooth-Earth surface must also be corrected:

$$m = \frac{h_{sr} - h_{st}}{d} \quad \text{m/km} \tag{141}$$

5.1.6.4 Terrain roughness, h_m

The terrain roughness parameter, h_m (m) is the maximum height of the terrain above the smooth-Earth surface in the section of the path between, and including, the horizon points:

$$h_m = \max_{i=i_{lt}}^{i_{lr}}\left[h_i - (h_{st} + m \cdot d_i)\right] \quad \text{m} \tag{142}$$

where:

i_{lt}: index of the profile point at distance d_{lt} from the transmitter

i_{lr}: index of the profile point at distance d_{lr} from the receiver.

The smooth-Earth surface and the terrain roughness parameter h_m are illustrated in Fig. 15.

FIGURE 15

An example of the smooth-Earth surface and terrain roughness parameter

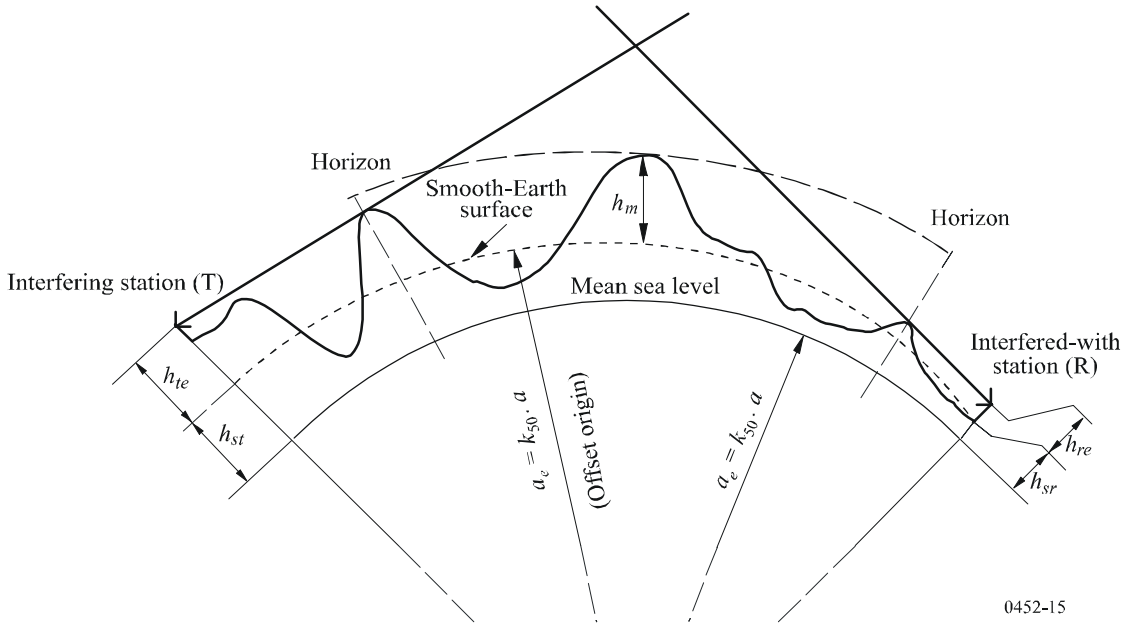

Appendix 3
to Annex 1

An approximation to the inverse cumulative normal distribution function for $x \leq 0.5$

The following approximation to the inverse cumulative normal distribution function is valid for $0.000001 \leq x \leq 0.5$ and is in error by a maximum of 0.00054. It may be used with confidence for the interpolation function in equation (13a). If $x < 0.000001$, which implies $\beta_0 < 0.0001\%$, x should be set to 0.000001. The function $I(x)$ is then given by:

$$I(x) = \xi(x) - T(x) \tag{143}$$

where:

$$T(x) = \sqrt{[-2\ln(x)]} \tag{143a}$$

$$\xi(x) = \frac{[(C_2 \cdot T(x) + C_1) \cdot T(x)] + C_0}{[(D_3 \cdot T(x) + D_2) T(x) + D_1] T(x) + 1} \tag{143b}$$

$$C_0 = 2.515516698 \tag{143c}$$

$$C_1 = 0.802853 \tag{143d}$$

$$C_2 = 0.010328 \tag{143e}$$

$$D_1 = 1.432788 \tag{143f}$$

$$D_2 = 0.189269 \tag{143g}$$

$$D_3 = 0.001308 \tag{143h}$$